

Network Group Hawkes Process Model

Haochen Xu¹, Guanhua Fang², and Xuening Zhu¹

¹*Fudan University, Shanghai, China;* ²*Columbia University, USA*

Abstract

In this work, we study the event occurrences of user activities on online social network platforms. To characterize the social activity interactions among network users, we propose a network group Hawkes (NGH) process model. Particularly, the observed network structure information is employed to model the users' dynamic posting behaviors. Furthermore, the users are clustered into latent groups according to their dynamic behavior patterns. To estimate the model, a constraint maximum likelihood approach is proposed. Theoretically, we establish the consistency and asymptotic normality of the estimators. In addition, we show that the group memberships can be identified consistently. To conduct estimation, a branching representation structure is firstly introduced, and a stochastic EM (StEM) algorithm is developed to tackle the computational problem. Lastly, we apply the proposed method to a social network data collected from Sina Weibo, and identify the influential network users as an interesting application.

KEY WORDS: Hawkes process; Point process; Social network analysis; Latent group; Stochastic EM.

*Haochen Xu and Guanhua Fang are joint first authors. Xuening Zhu (xueningzhu@fudan.edu.cn) is the corresponding author. This work is supported by the National Natural Science Foundation of China (nos. 11901105, 71991472, 11971504, U1811461), the Shanghai Sailing Program for Youth Science and Technology Excellence (19YF1402700), and the Fudan-Xinzailing Joint Research Centre for Big Data, School of Data Science, Fudan University.

1. INTRODUCTION

Consider a network with m nodes, which are indexed as $i = 1, \dots, m$. To characterize the relationship among the nodes, we employ an adjacency matrix $A = (a_{ij}) \in \mathbb{R}^{m \times m}$, where $a_{ij} = 1$ implies that the i th node follows the j th node, otherwise $a_{ij} = 0$. Following the convention, we do not allow self-connected nodes, i.e., $a_{ii} = 0$. For the i th node, we collect a number of events occurring at time points $0 \leq t_{i1} \leq t_{i2} \leq \dots \leq t_{in_i} \leq T$. For instance, on an online social network, one can record the time stamps of user posts, comments, and many other user dynamic behaviors. Developing statistical tools to model the dynamic patterns of these events is critical for making decisions (Srijith et al., 2017; Sayyadi et al., 2009; Liu et al., 2012).

To motivate the research idea, we first conduct a preliminary analysis using user posting dataset collected from Sina Weibo (the largest Twitter type social media platform in mainland China). The dataset contains 2038 users, whose posting behaviors are collected during the period from January 1st to January 15th, 2014. First, we calculate the time intervals between two subsequent Weibo posts for the same user i (i.e., $t_{i(k+1)} - t_{ik}$). The histogram of all time intervals is shown in the left panel of Figure 1. As implied by Figure 1, more than 60% Weibo posts occur within 1 hour to the user’s last post. This indicates the user posting times are highly clustered. Next, for each posting time t_{ik} of user i , we calculate the time interval to the latest post from the user’s connected friends (i.e., $\min_{j,l} \{t_{ik} - t_{jl} I(a_{ij} = 1, t_{jl} < t_{ik})\}$). This leads to the histogram in the right panel of Figure 1. Similarly, a spike in shorter time intervals can be observed. This evidence suggests that the network users might have active interactions with their following friends. Lastly, we draw hourly posts of three representative users in Figure 2. As one could observe, the posting behaviors of the three users exhibit quite different patterns. For instance, the account “Movie View” tends to post around 9:00 am while the account “Toutiao” is more active in the afternoon. Therefore, beyond the clustering effects, the network users also have distinct dynamic patterns.

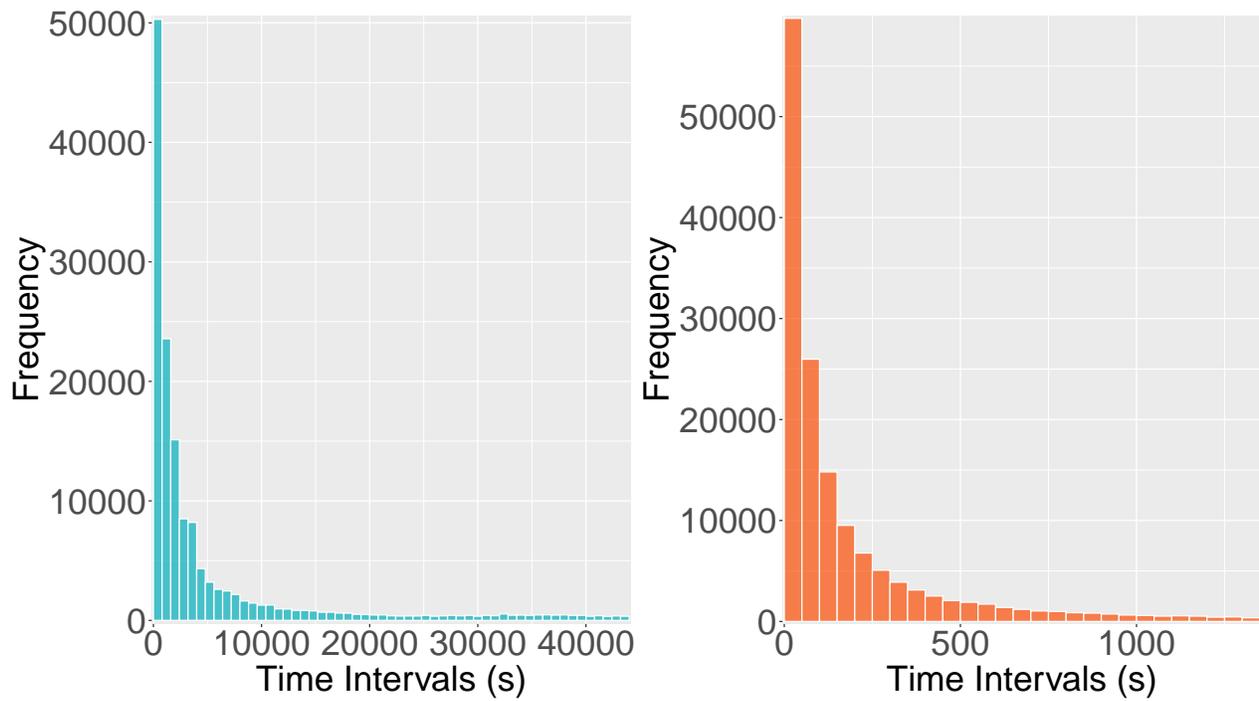


Figure 1: The histogram of time intervals between Weibo posts. The left panel: histogram of the time intervals between two subsequent Weibo posts for each individual; the right panel: histogram of the time intervals between user-self posts and the latest posts from their connected friends.

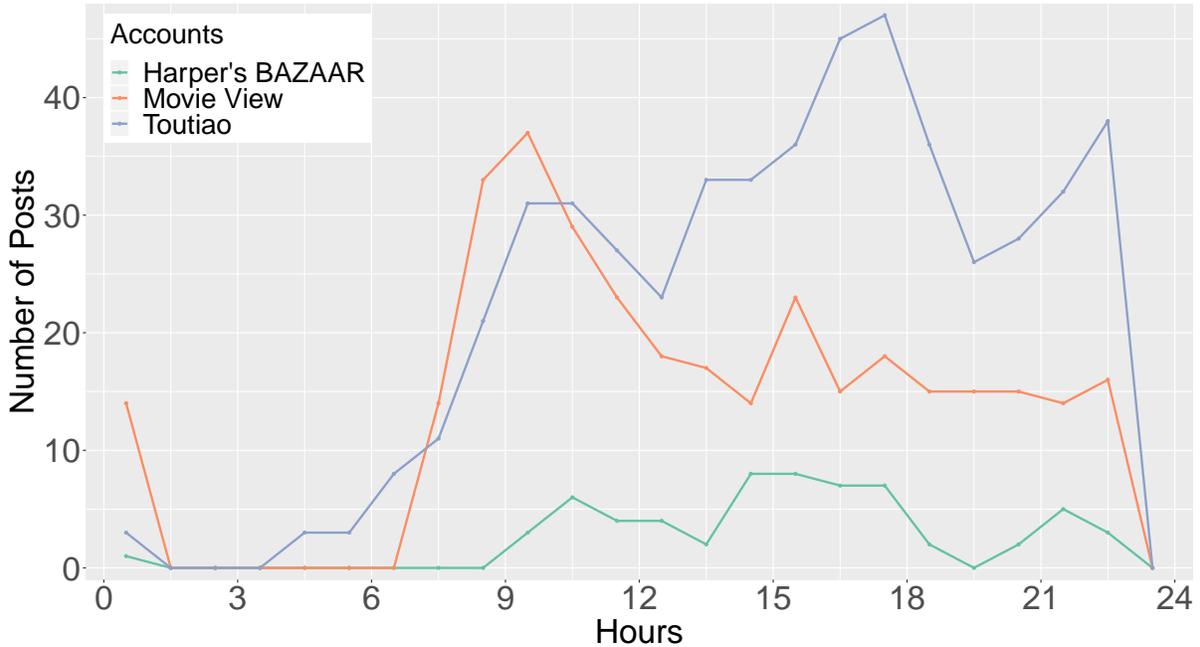


Figure 2: Hourly users’ posts from three typical users (“Movie View”, “Toutiao” and “Harper’s BAZAAR”) in the Sina Weibo dataset. The number of posts within each hour is aggregated for the 15 days from January 1st to January 15th, 2014.

The above preliminary analysis motivates us to model the occurrences of event using a clustered point process. In this regard, two common wisdoms exist. The first approach is to model each user separately by using a univariate clustered point process. In this aspect, the Hawkes process (Hawkes and Oakes, 1974) is one of the widely used approaches in the literature. For instance, in seismology study, the Hawkes process is used to describe earthquake occurrences (Veen and Schoenberg, 2008). The similar modeling framework has also been introduced to model urban crime patterns (Mohler et al., 2011) and conversation sequences (Masuda et al., 2013). Despite the usefulness of this approach, the cross-sectional information among different users might be ignored. As an alternative, one could consider to employing a multivariate Hawkes process model (Hawkes, 1971). For example, Fox et al. (2016) applies the multivariate Hawkes process model to an e-mail network dataset. However, estimating the model requires to estimate $O(m^2)$ pairwise interaction parameters, which leads to a heavy computational burden and thus cannot be directly applied to large scale networks.

To our best knowledge, none of the above works have taken the observed network information (i.e., A) into consideration. In this work, we propose a network group Hawkes (NGH) process model, where we explicitly embed the network information into the modeling framework. In addition, the nodes are assigned to several latent groups according to their dynamic behavior patterns. Specifically, we model the intensity function of each node as a linear combination of the following three parts: (1) baseline intensity, which reflects daily periodic activities of the nodes, (2) momentum intensity, which characterizes the influence of the node’s historical events to the current event, and (3) network intensity, which captures the influences of the node’s connected friends. In addition, we allow each node with a latent group membership, where in each group the nodes exhibit the same dynamic behavior patterns.

Statistically, the dynamic patterns of the network nodes are specified by a set of group leveled parameters. Compared to the multivariate Hawkes process, the number of parameters to be estimated is largely reduced. To estimate the model, we propose a constraint maximum likelihood estimator (CMLE), whose asymptotic properties are investigated. In addition, the consistency result of the group membership estimation is established.

Numerically, we further develop a stochastic EM (StEM) algorithm for model estimation. The EM-type algorithm is firstly introduced by Veen and Schoenberg (2008) for Hawkes process estimation and then widely applied (Halpin et al., 2013; Fox et al., 2016). In this work, we revise the conventional EM algorithm to a stochastic version to further reduce the computational burden. Specifically, a branching representation of the NGH process is firstly introduced and then the StEM algorithm is presented. Extensive numerical studies are conducted to verify the robustness and accuracy of the algorithm. Lastly, we conduct an empirical study using data collected from Sina Weibo platform. Specifically, a user profile analysis is conducted according to the model estimation result. In addition, the influential powers of network users are analyzed based on their abilities to influence others.

The rest of the article is organized as follows. In Section 2, we introduce notations and the

network group Hawkes (NGH) process model. In Section 3, we provide the estimation methods and the corresponding theoretical properties. The branching representation structure and the stochastic EM algorithm are described in Section 4. The simulation results under different network settings are presented in Section 5. In Section 6, we apply the proposed method to a Sina Weibo dataset for user analysis. The article is concluded with a brief discussion in Section 7. All technical details are left to the Appendix and separate supplementary material.

2. HAWKES PROCESS FOR NETWORK DATA

2.1. Introduction to Hawkes Process

Before introducing the model, we briefly review several necessary preliminaries of the Hawkes process. Hawkes process is a widely used self-exciting point process (Hawkes and Oakes, 1974) that models the occurrences of events through the intensity function. Consider a temporal point process of event times $0 \leq t_1 \leq t_2 \leq \dots \leq t_n \leq T$ within $[0, T]$. In general, we use $N(t) = \sum_{k=1}^n \mathbb{I}\{t_k < t\}$ to denote event counts within time period $[0, t]$. Let $\mathcal{H}_t = \{t_k : t_k < t\}$ be the history information up to time t , then the conditional intensity function is defined as

$$\lambda(t|\mathcal{H}_t) = \lim_{\Delta \rightarrow 0} \frac{\mathbb{E}[N\{[t, t + \Delta)\}|\mathcal{H}_t]}{\Delta}.$$

The classical Hawkes process models the conditional intensity function as

$$\lambda(t|\mathcal{H}_t) = \nu + \sum_{t_k < t} f(t - t_k), \tag{2.1}$$

where $\nu > 0$ denotes a constant background rate of events, and $f(\cdot)$ is a triggering function which specifies the influences of the historical events to the current time (Chen et al., 2017). The process is referred to as “self-exciting” process because the conditional intensity function depends on historical events through the triggering function $f(\cdot)$. By choosing the form of $f(\cdot)$, one could specify whether the process depends mainly on recent history or has a long memory.

2.2. Network Group Hawkes Process

In this section, we extend the original Hawkes process to a network group Hawkes process, which is used to model the temporal point processes of network users. Recall that m is the network size and for the i th node we could collect the event times $\{t_{ik} : 1 \leq k \leq n_i\}$. Accordingly, define $N_i(t) = \sum_{k=1}^{n_i} \mathbf{I}(t_{ik} \leq t)$ as the number of events for the user i up to time t . Furthermore, we assume the nodes are collected from G latent groups. Within each group, the nodes are assumed to share the same set of group-level parameters. Specifically, for the i th node, let $g_i \in \{1, \dots, G\}$ denote the group membership of the user i . Suppose the latent membership g_i follows a categorical distribution, i.e., $g_i \sim \text{Cat}(\{1, 2, \dots, K\}, \pi)$, where $\pi = (\pi_1, \dots, \pi_G)^\top$ is the group prior probability. Let $\mathcal{G} = (g_1, \dots, g_m)^\top \in \mathbb{R}^m$ be the latent group vector which collects the group memberships of all users.

Given the latent group vector \mathcal{G} and all history information $\mathcal{H}_t = \{t_{ik} : t_{ik} < t; 1 \leq k \leq n_i, 1 \leq i \leq m\}$, we characterize the conditional intensity function for the i th node by the following network group Hawkes (NGH) process model,

$$\lambda_i(t|\mathcal{G}) = \mu_{g_i}(t) + \beta_{g_i} \sum_{t_{ik} < t} f(t - t_{ik}; \eta_{g_i}) + \sum_{j=1}^m \alpha_{g_i g_j} \frac{a_{ij}}{d_i} \sum_{t_{jl} < t} f(t - t_{jl}; \gamma_{g_i}), \quad (2.2)$$

where $\mu_g(t)$ is a baseline function, $f(t; \gamma)$ is a triggering function, $d_i = \sum_j a_{ij}$ is the out-degree for node i , and $\{\beta_g, \gamma_g, \eta_g, \alpha_{gg'}\}$ are unknown group-level parameters. Specifically, the conditional intensity in (2.2) of the node i constitutes of three parts. The first part $\mu_{g_i}(t)$ is referred to as a *baseline intensity*. We assume that the baseline intensity $\mu_g(t)$ approximately takes a periodic form, which represents the daily periodic behaviors of the network users. Next, the second part $\beta_{g_i} \sum_{t_{ik} < t} f(t - t_{ik}; \eta_{g_i})$ takes a standard self-exciting process form, which reflects the influences of the node's own historical events. Therefore, we refer to it as *momentum intensity*. Usually the triggering function $f(t - s; \gamma)$ is specified as a decaying function of $(t - s)$, where γ is the parameter controlling decaying rate. Lastly, the third part $\sum_{j=1}^m \alpha_{g_i g_j} d_i^{-1} a_{ij} \sum_{t_{jl} < t} f(t - t_{jl}; \gamma_{g_i})$ is a weighted average of triggering functions from the node's following friends. We refer to this part as *network*

intensity. Note that with respect to the j th user, the weight is specified by $\alpha_{g_i g_j} d_i^{-1} a_{ij}$. Hence, only the following friends (i.e., $\{j : a_{ij} \neq 0\}$) have influences on the current node. This also makes sense in practice because on a social network platform, only the following friends are visible to the focal user. In addition, if the i th node follows the j th node (i.e., $a_{ij} = 1$), then the weight is decided by both their group connection strength (i.e., $\alpha_{g_i g_j}$) and the out-degree of the i th node (i.e., d_i).

Remark 1. (Comparison with the NAR Model) In a recent work of Zhu et al. (2017), a network vector autoregression (NAR) model was proposed to model the time series dynamics for network users. Suppose we could collect a continuous type response Y_{it} for the i user at the t th time point. Then the NAR model takes the following form,

$$Y_{it} = \beta_{0i} + \beta_1 d_i^{-1} \sum_j a_{ij} Y_{j(t-1)} + \beta_2 Y_{i(t-1)} + \varepsilon_{it}, \quad (2.3)$$

where ε_{it} is a random noise term. The proposed NGH process shares wisdom with the NAR model (2.3) by explicitly exploiting the known network information. In the meanwhile, the proposed framework could model more detailed temporal point process patterns for network users, while the NAR model is only suitable for modeling discrete time dynamics at an aggregated level.

3. PARAMETER ESTIMATION

3.1. Periodic Baseline Intensity Function

In the original Hawkes process model (2.1), the background rate is assumed to be a stationary Poisson process. In practice, however, this might not be true due to the periodic rhythms of human activities (Cho et al., 2011). This phenomenon is also supported by our social media data. Particularly, we aggregate all users' posts within every 6 hours from January 1st to January 15th in 2014, which leads to the barplot in Figure 3. A clear periodic pattern can be observed. This motivates us to consider a periodic baseline intensity function form.

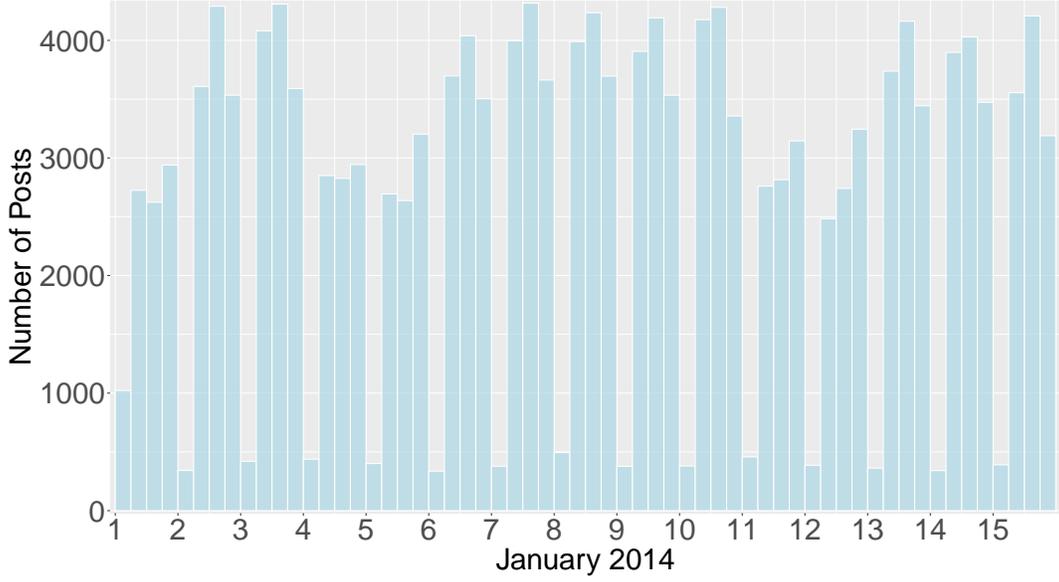


Figure 3: The barplot of posts in every 6 hours from January 1st to 15th, 2014 for the Sina Weibo dataset.

Let $\omega \in \mathbb{R}$ be the period of the baseline intensity function. Consider a set of basis functions $\Phi_b = \{k_j(t) : t \in [0, \omega), 1 \leq j \leq n_b\}$. Correspondingly, define a functional space $\mathcal{F} = \{f(t)\}$, where $f(t)$ takes a periodic form with period ω as

$$f(t) = \begin{cases} \sum_{j=1}^{n_b} w_j k_j(t), & \text{if } t \in [0, \omega) \\ f(t - n\omega), & \text{if } t \in [n\omega, (n+1)\omega), n \geq 1. \end{cases} \quad (3.1)$$

In the following we define the functional norm of $f(t)$ ($t \in [0, T]$) as $\|f(t)\|_\infty = \sup_{t \in [0, T]} |f(t)|$. We state the following assumption for the baseline intensity function.

(C1) (BASELINE INTENSITY ASSUMPTION) Let the true baseline function $\mu_g^*(t)$ be a periodic function with period ω . In addition, it satisfies

$$\min_g \inf_{f \in \mathcal{F}} \|\mu_g^* - f\|_\infty = O(n_b^{-r}), \quad (3.2)$$

where $r \geq 2$ is a constant. Here the basis functions $k_j(t)$ for constructing $f(t)$ in (3.1) satisfy:

(a) $\int_0^\omega k_j(t) dt = O(n_b^{-1})$ and $\|k_j(t)\|_\infty < \infty$, and (b) $\int_0^\omega k_j(t) k_{j+l}(t) dt \leq \exp(-cl)$ for $l \leq J$ and

$k_j(t)k_{j+l}(t) = 0$ for $l > J$, where $J \geq 0$ is a finite integer and c is a positive constant.

The above condition specifies an approximated periodic form for the baseline intensity function $\mu_g^*(\cdot)$ by (3.2). Particularly, the conditions for the basis functions $k_j(t)$ guarantee that they are well separated from each other. It is remarkable that we do not restrictively require $\mu_g^* \in \mathcal{F}$ but just assume μ_g^* “approximates” \mathcal{F} with approximation error n_b^{-r} , which is more flexible and easy to satisfy in practice.

Remark 2. (Comparison with E-mail Network Self-Exciting Process) In a recent work by Fox et al. (2016), they consider to model e-mail traffic network by using the following intensity function,

$$\lambda_i(t) = \nu_i \mu(t) + \sum_{t_{ik} < t} g_i(t - t_{ik}),$$

where ν_i is a user-specific parameter and $\mu(t)$ is a baseline density function accounting for users’ periodic activities. With regards to the formulation of the baseline intensity function, we extend the above approach in the following two directions. First, instead of specifying an individualized parameter ν_i , we assume the baseline intensity is group-specific. Therefore, we could aggregate information from all users within the same group to enhance estimation accuracy. Second, the baseline intensity function is assumed to “approximately” take a linear combination of basis functions. Hence it will be able to characterize more flexible function forms.

3.2. Constrained Maximum Likelihood Estimator

Given the assumption of the baseline intensity function, we discuss the estimation of the NGH process. To estimate the intensity function $\lambda_i(t|\mathcal{G})$, a classical approach is to use the maximum likelihood estimation. Let $\theta_g = (\beta_g, \eta_g, \gamma_g)^\top \in \mathbb{R}^3$ and $\alpha = (\alpha_{ij} : 1 \leq i, j \leq G) \in \mathbb{R}^{G \times G}$. Denote the group-level parameters as $\Theta = (\Theta_j)^\top = (\theta_1^\top, \dots, \theta_G^\top, \text{vec}(\alpha)^\top)^\top \in \mathbb{R}^q$, where $q = 3G + G^2$. In addition, define the set of baseline intensity functions as $\mathbb{U} = \{\mu_1, \dots, \mu_g\}$.

For the NGH process, the complete-data likelihood function takes the form as

$$\begin{aligned} L_{com}(\Theta, \mathbb{U}, \pi, \mathcal{G}) &= \prod_{i=1}^m \pi_{g_i} \exp \left\{ \int \log \lambda_i(t|\mathcal{G}) dN_i(t) - \Lambda_i(T|\mathcal{G}) \right\} \\ &= \prod_{i=1}^m \prod_{g=1}^G \left\{ \pi_g \prod_{k=1}^{n_i} \lambda_i(t_{ik}|\mathcal{G}) \exp(-\Lambda_i(T|\mathcal{G})) \right\}^{I(g_i=g)}, \end{aligned} \quad (3.3)$$

where $\Lambda_i(T|\mathcal{G}) = \int_0^T \lambda_i(t|\mathcal{G}) dt$. By integrating the complete-data likelihood (3.3) with respect to the latent membership \mathcal{G} , we could obtain the following marginal likelihood function as

$$L_{mar}(\Theta, \mathbb{U}, \pi) = \sum_{g_1=1}^m \sum_{g_2=1}^m \cdots \sum_{g_m=1}^m \left[\prod_{i=1}^m \left\{ \pi_{g_i} \prod_{k=1}^{n_i} \lambda_i(t_{ik}|\mathcal{G}) \exp(-\Lambda_i(T|\mathcal{G})) \right\} \right]. \quad (3.4)$$

The maximum likelihood estimator is then given by $(\hat{\Theta}_{mle}, \hat{\mathbb{U}}_{mle}, \hat{\pi}_{mle}) = \arg \max L_{mar}(\Theta, \mathbb{U}, \pi)$.

Although the above maximum likelihood estimation framework is straightforward, it is still hard to obtain $\hat{\mathbb{U}}_{mle}$ since the baseline intensity functions could take any flexible forms. Recall that we assume the baseline intensity functions could be approximately expressed by a linear combination of a set of basis functions in Condition (C1). Therefore, we could constrain $\mu_g \in \mathcal{F}$ and estimate $\mu_g(t)$ as linear combination of basis functions in Φ_b . This is computationally feasible since only the coefficients of the basis functions, i.e., w_j , need to be estimated.

Correspondingly, denote $L_c(\Theta, \mathbb{U}, \pi) = L_{mar}(\Theta, \mathbb{U}, \pi; \mu_g \in \mathcal{F})$ as constrained likelihood function by restricting $\mu_g \in \mathcal{F}$. We then have the following constrained maximum likelihood estimator (CMLE),

$$(\hat{\Theta}_{cmle}, \hat{\mathbb{U}}_{cmle}, \hat{\pi}_{cmle}) = \arg \max_{(\Theta, \mathbb{U}, \pi)} L_c(\Theta, \mathbb{U}, \pi). \quad (3.5)$$

Next, we plug-in the CMLE into the complete-data likelihood function (3.3) to obtain the group membership estimation, i.e., $\hat{\mathcal{G}} = \arg \max_{\mathcal{G}} L_{com}(\hat{\Theta}_{cmle}, \hat{\mathbb{U}}_{cmle}, \hat{\pi}_{cmle}, \mathcal{G})$. In the following section, we further investigate the theoretical properties of the proposed estimators.

3.3. Theoretical Properties

In this section, we discuss the theoretical properties of the proposed estimation method of the NGH process. First, we establish the consistency and asymptotic normality result for the parameter estimation. Second, we establish the consistency of group membership estimation and provide a criterion for choosing the number of groups.

Let $\Theta^*, \mathbb{U}^*, \pi^*$ and \mathcal{G}^* denote the true parameters and group membership vector. Following Zhao et al. (2012), we define a group membership estimation criterion Q to be consistent if the group labels obtained by maximizing the criterion Q , $\hat{\mathcal{G}} = \arg \max_{\mathcal{G}} Q(\mathcal{G})$, satisfying

$$P(\hat{\mathcal{G}} = \mathcal{G}) \rightarrow 1 \quad \text{as } \min\{m, T\} \rightarrow \infty. \quad (3.6)$$

Clearly, the above definition has identification issues. Strictly speaking, a reasonable criterion should stay invariant under a permutation of group labels $\{1, \dots, G\}$. Therefore, it is better to require that $\hat{\mathcal{G}}$ and \mathcal{G} belong to the equivalent class under label permutations. For notation simplicity, in the following, we still write $\hat{\mathcal{G}} = \mathcal{G}$ to represent that $\hat{\mathcal{G}}$ and \mathcal{G} are equal up to a permutation of labels. Similarly, $\hat{\mathcal{G}} \neq \mathcal{G}$ means $\hat{\mathcal{G}}$ and \mathcal{G} are not equivalent to any permutation of labels.

Define $\lambda_i^*(t|\mathcal{G}^*)$ as the true intensity function. In addition, let $\ell_c(\Theta, \mathbb{U}, \pi) = \log L_c(\Theta, \mathbb{U}, \pi)$ as the log constrained likelihood function. Specifically, for any vector $v = (v_i)^\top$, define $\|v\|_\infty = \max_i |v_i|$. For an arbitrary matrix $M = (m_{ij}) \in \mathbb{R}^{p_1 \times p_2}$, let $\|M\|_\infty = \max_i |\sum_j m_{ij}|$. To establish the estimation properties of the parameters, we require the following conditions.

(C2) (PARAMETER SPACE) Assume the parameter space is convex, i.e., $\|\Theta\|_\infty \leq C_0$, and Θ^* lies in the interior of the convex set, where C_0 is a finite positive constant. In addition, assume $\Theta_j > 0$ for $1 \leq j \leq q$. For the baseline intensity function, further assume $\max_g \|\mu_g\|_\infty \leq C_0$ and $\min_g \inf_t \mu_g(t) \geq C_1$, where $C_1 \leq C_0$ is a positive constant.

(C3) (STATIONARITY) Define $b_{ij} = \alpha_{g_i, g_j}^* d_i^{-1} a_{ij} + \beta_{g_i}^* I(i = j)$ and $B = (b_{ij}) \in \mathbb{R}^{m \times m}$. Assume

$\|B\|_\infty \leq c_B < 1$, where c_B is a positive constant. Further assume the triggering function $f(t; \gamma)$ satisfies: (1) $f(t; \gamma) \leq c_f \gamma \exp(-\gamma t)$ for any $t \in [0, T]$, and (2) $\lim_{t \rightarrow \infty} f(t; \gamma) / \exp(-\gamma t) \rightarrow 0$, where c_f is a positive constant.

(C4) (NETWORK DEGREE) Let $d_{out, \min} = \min_i \sum_j a_{ij}$ and $d_{in, \max} = \max_j \sum_i a_{ij}$ be the minimum out-degree and maximum in-degree. Assume $d_{gap} \stackrel{\text{def}}{=} d_{in, \max} / d_{out, \min} = m^{r_d}$, where $r_d \in (0, 1)$ is a constant.

(C5) (LOCAL CONVEXITY) Suppose $\ell_c(\Theta, \mathbb{U}, \pi)$ has continuous second order derivatives with respect to Θ and μ_g ($1 \leq g \leq G$), where the functional derivative is defined in Definition 1 in Appendix A.1. Define

$$\begin{aligned} \mathcal{I}_{11} &= \frac{1}{mT} E \left[\frac{\partial^2 \ell_c(\Theta^*, \mathbb{U}^*, \pi^*)}{\partial \Theta \partial \Theta^\top} \right] \in \mathbb{R}^{q \times q}, \\ \mathcal{I}_{12} &= \frac{1}{mT} E \left[\frac{\partial^2 \ell_c(\Theta^*, \mathbb{U}^*, \pi^*)}{\partial \Theta \partial \mu_g^\top} \right]_{1 \leq g \leq G} \in \mathbb{R}^{q \times (n_b G)}, \\ \mathcal{I}_{22} &= \frac{1}{mT} E \left[\frac{\partial^2 \ell_c(\Theta^*, \mathbb{U}^*, \pi^*)}{\partial \mu_{g_1} \partial \mu_{g_2}^\top} \right]_{1 \leq g_1, g_2 \leq G} \in \mathbb{R}^{(n_b G) \times (n_b G)} \end{aligned}$$

and $\mathcal{I}_{21} = \mathcal{I}_{12}^\top$. Assume $\Sigma_{2\Theta} \stackrel{\text{def}}{=} \lim_{m, T \rightarrow \infty} (\mathcal{I}_{11} - \mathcal{I}_{12} \mathcal{I}_{22}^{-1} \mathcal{I}_{21}) \in \mathbb{R}^{q \times q}$ exists and is positive definite. In addition assume a similar local convexity condition (C5.a) in Appendix A.1.

(C6) (CONVERGENCE) Define

$$\mathcal{S}_1 = \frac{\partial \ell_c(\Theta^*, \mathbb{U}^*, \pi^*)}{\partial \Theta} \in \mathbb{R}^q, \quad \mathcal{S}_2 = \left[\frac{\partial \ell_c(\Theta^*, \mathbb{U}^*, \pi^*)^\top}{\partial \mu_g} \right]_{1 \leq g \leq G}^\top \in \mathbb{R}^{n_b G}.$$

Assume there exists a sequence $\{d_m\}$ such that $\Sigma_{1\Theta} \stackrel{\text{def}}{=} \lim_{m, T \rightarrow \infty} (mT d_m)^{-1} \text{cov}(\mathcal{S}_1 - \mathcal{I}_{12} \mathcal{I}_{22}^{-1} \mathcal{S}_2) \in \mathbb{R}^{q \times q}$ exists and $\Sigma_{1\Theta}$ is positive definite.

We make comments on the above conditions. Condition (C2) is a regular condition which assumes that the parameter space is compact and convex, and the true parameter is an interior point. This type of condition is widely assumed in literature (Van der Vaart, 2000; Fan and Li,

2001; Wang et al., 2017). Condition (C3) is a stationary type condition, which is also made for multivariate stationary Hawkes process (Gao and Zhu, 2018). It guarantees that the process will not explode as $T \rightarrow \infty$. Furthermore, we would like to remark that although the requirement on the triggering function $f(t; \gamma)$ is sufficient for model stationarity, it is not a necessary condition in practice. Typically, the triggering function is set in the form $f(t; \gamma) = \gamma \exp(-\gamma t)$ in practice in order to obtain analytical solutions in parameter estimation, and this is also shown to have good finite sample performance (Halpin et al., 2013). Condition (C4) is imposed on the network degrees. Specifically, it restricts that the unbalance effect of network nodes should not be too large. Lastly, Conditions (C5) and (C6) are regular conditions that are widely assumed in literature (He and Shi, 1996; Lehmann and Casella, 2006; Fan et al., 2007; Sit et al., 2018). Specifically, Condition (C5) ensures that Θ^* is a local minimum of the population objective function $E\{\ell_c(\Theta^*, \mathbb{U}^*, \pi^*)\}$. Condition (C6) is a convergence condition, which specifies the rates of convergence and leads to the asymptotic normality result.

Next, we discuss the identification conditions of the proposed method. Note that the marginal likelihood function is defined by assuming the true number of groups G is known. However, in practice, we may suffer from the mis-specification problem. Particularly, given any number of groups G' , we could correspondingly define the marginal likelihood function as $L_{mar}^{(G')}(\Theta, \mathbb{U}, \pi)$ and $\ell_{mar}^{(G')}(\Theta, \mathbb{U}, \pi) = \log\{L_{mar}^{(G')}(\Theta, \mathbb{U}, \pi)\}$. Then the following condition is assumed to make sure that the true parameters $(\Theta^*, \mathbb{U}^*, \pi^*)$ can be uniquely identified, and the group number G can be consistently selected.

(C7) (MODEL IDENTIFICATION) Assume $\bar{\ell}_{mar}^{(G')}(\Theta, \mathbb{U}, \pi) = \lim_{m, T \rightarrow \infty} (mT)^{-1} E\{\ell_{mar}^{(G')}(\Theta, \mathbb{U}, \pi)\}$ exists and $\bar{\ell}_{mar}^{(G')}(\Theta, \mathbb{U}, \pi)$ is a continuous function of Θ , π , and $\mu_g(t)$ ($1 \leq g \leq G'$) given any G' . Here the continuity of $\bar{\ell}_{mar}^{(G')}(\Theta, \mathbb{U}, \pi)$ with respect to function $\mu_g(t)$ is defined in Definition 2 in Appendix A.1.

(C7.1) Assume $\bar{\ell}_{mar}^{(G)}(\Theta, \mathbb{U}, \pi)$ admits a unique global maximizer at $(\Theta^*, \mathbb{U}^*, \pi^*)$, i.e., for any $(\Theta, \mathbb{U}, \pi) \neq (\Theta^*, \mathbb{U}^*, \pi^*)$ we have $\bar{\ell}_{mar}^{(G)}(\Theta^*, \mathbb{U}^*, \pi^*) > \bar{\ell}_{mar}^{(G)}(\Theta, \mathbb{U}, \pi)$. Assume there exists

$\delta > 0$, for any π satisfying $\|\pi - \pi^*\|_2 \leq \delta$, it holds $\bar{\ell}_{mar}^{(G)}(\Theta^*, \mathbb{U}^*, \pi) - \delta_1 R(\Theta, \mathbb{U}, \pi)^2 \leq \bar{\ell}_{mar}^{(G)}(\Theta, \mathbb{U}, \pi) \leq \bar{\ell}_{mar}^{(G)}(\Theta^*, \mathbb{U}^*, \pi) - \delta_2 R(\Theta, \mathbb{U}, \pi)^2$ with $(0 < \delta_2 < \delta_1 < \infty)$, where $R(\Theta, \mathbb{U}, \pi) = \max\{\|\Theta - \Theta^*\|_\infty, \max_g \|\mu_g - \mu_g^*\|_\infty\}$.

(C7.2) For any underfitted model with $G_- < G$, there exists a finite constant $c > 0$, such that $\sup_{(\Theta, \mathbb{U}, \pi)} \bar{\ell}_{mar}^{(G_-)}(\Theta, \mathbb{U}, \pi) < \bar{\ell}_{mar}^{(G)}(\Theta^*, \mathbb{U}^*, \pi^*) - c$.

Condition (C7.1) ensures that the true parameter could be uniquely identified when the true number of groups G is known in a population level. Specifically, we remark that the inequality $(\Theta, \mathbb{U}, \pi) \neq (\Theta^*, \mathbb{U}^*, \pi^*)$ means that the inequivalence of the parameter sets under group label permutations. In addition, $\bar{\ell}_{mar}^{(G)}(\Theta, \mathbb{U}, \pi)$ is assumed to have a local quadratic form around $(\Theta^*, \mathbb{U}^*, \pi)$. Next, Condition (C7.2) guarantees that a sufficiently large gap should exist between the true model $\bar{\ell}_{mar}^{(G)}(\Theta^*, \mathbb{U}^*, \pi^*)$ and an underfitted model $\bar{\ell}_{mar}^{(G_-)}(\Theta, \mathbb{U}, \pi)$. Consequently, the true number of groups G can be consistently selected.

Similarly, to uniquely identify the group membership \mathcal{G}^* , we define $\ell_{com}(\Theta, \mathbb{U}, \pi, \mathcal{G}) = \log\{L_{com}(\Theta, \mathbb{U}, \pi, \mathcal{G})\}$ and assume the following condition.

(C8) (GROUP MEMBERSHIP IDENTIFICATION) Assume $\bar{\ell}_{com,m}(\Theta, \mathbb{U}, \pi, \mathcal{G}) = \lim_{T \rightarrow \infty} (mT)^{-1} E\{\ell_{com}(\Theta, \mathbb{U}, \pi, \mathcal{G}) | \mathcal{G}\}$ exists for any \mathcal{G} . Assume there exists an $m_0 > 0$ and $c > 0$, for any $m > m_0$, it holds

$$\sup_{(\Theta, \mathbb{U}, \pi, \mathcal{G}) \neq (\Theta^*, \mathbb{U}^*, \pi^*, \mathcal{G}^*)} \bar{\ell}_{com,m}(\Theta, \mathbb{U}, \pi, \mathcal{G}) < \bar{\ell}_{com,m}(\Theta^*, \mathbb{U}^*, \pi^*, \mathcal{G}^*) - c,$$

where the inequality $(\Theta, \mathbb{U}, \pi, \mathcal{G}) \neq (\Theta^*, \mathbb{U}^*, \pi^*, \mathcal{G}^*)$ is defined under group label permutations.

Similar to Condition (C7), Condition (C8) further ensures that the group memberships can be identified. Given the above assumptions, we establish the parameter estimation consistency in the following theorem.

Theorem 1. (CONSISTENCY) *Assume Conditions (C1)–(C5) and (C8). In addition assume $n_b \ll \min\{T^{1-\delta}/m^{2r_d+11}, (T^{1-\delta}/m^{r_d})^{1/3}\}$ with $0 < \delta < 1$. Then we have the following result,*

$$\widehat{\Theta}_{cmle} \rightarrow_p \Theta^* \quad \text{and} \quad \max_g \|\widehat{\mu}_{cmle,g} - \mu_g^*\|_\infty \rightarrow_p 0. \quad (3.7)$$

The proof of Theorem 1 is given in Appendix B.1. Note that the consistency requires that the number of basis functions n_b is not too large. Specifically, it should be smaller as the total time periods T is shorter and the network is more unbalanced (i.e., m^{r_d} is higher). Particularly, if we assume a truncated form for the triggering function, i.e., $f(t; \gamma) = 0$ for $t \geq C$ (C is some finite constant), we could relax the upper bound on n_b further. Next, the following corollary establishes the convergence rates of $\widehat{\Theta}_{cmle}$ and $\widehat{\mu}_{cmle,g}$ respectively.

Corollary 1. *Assume Conditions (C1)–(C5) and (C8). In addition, assume $n_b \ll \min\{T^{1-\delta}/m^{2r_d+11}, (T^{1-\delta}/m^{r_d})^{1/(1+2r)}\}$ with $0 < \delta < 1$. Then we have*

$$P\left[\frac{1}{mT} \sum_i \int_0^T \{\widehat{\lambda}_i(t|\mathcal{G}^*)^{1/2} - \lambda_i^*(t|\mathcal{G}^*)^{1/2}\}^2 dt \geq \epsilon\right] < \frac{C}{T}, \quad (3.8)$$

$$\|\widehat{\Theta}_{cmle} - \Theta^*\|_\infty = O_p(n_b^{-r}) \quad \text{and} \quad \max_g \|\widehat{\mu}_{cmle,g} - \mu_g^*\|_\infty = O_p(n_b^{1-r}). \quad (3.9)$$

The proof of Corollary 1 is given in Appendix B.2. It suggests that the convergence rate of $\widehat{\Theta}_{cmle}$ can be as fast as n_b^{-r} , which is the approximation error in Condition (C1). Beyond the consistency result, we could further obtain the following asymptotic normality property.

Theorem 2. (ASYMPTOTIC NORMALITY) *Assume Conditions (C1)–(C8), and the conditions in Theorem 1. In addition assume $n_b^{-r} = o(d_m^{1/2} m^{-9/2-r_d} T^{-1/2-\delta})$, where $\delta > 0$ is a positive constant. Then we have*

$$\sqrt{\frac{mT}{d_m}} (\widehat{\Theta}_{cmle} - \Theta^*) \rightarrow_d N(\mathbf{0}, \Sigma_{2\Theta}^{-1} \Sigma_{1\Theta} \Sigma_{2\Theta}^{-1}).$$

The proof of Theorem 2 is provided in Appendix B.3. It further requires that the approximation error (i.e., n_b^{-r}) should be small enough to be ignored. Therefore the asymptotic normality could

hold. Besides the parameter estimation consistency, we further establish the group membership consistency in the following theorem.

Theorem 3. (GROUP MEMBERSHIP ESTIMATION) *Assume the same conditions in Theorem 1 and the number of groups G is correctly specified. Then we have $P(\hat{\mathcal{G}} = \mathcal{G}^*) \rightarrow 1$ as $m, T \rightarrow \infty$.*

The proof of Theorem 3 is given in Appendix B.4. Note that Theorem 3 is established based on the condition that G is correctly specified. Therefore, it is of great importance to decide the number of groups in practice. To this end, we propose a likelihood-based information criterion (LIC) in the following theorem, which is able to select the true number of groups G consistently.

Theorem 4. *Assume the same conditions with Corollary 1. Define a likelihood based information criterion (LIC) as*

$$LIC_G = \ell_{mar}^{(G)}(\hat{\Theta}^{(G)}, \hat{\mathbb{U}}^{(G)}, \hat{\pi}^{(G)}) - \lambda_{mT}G, \quad (3.10)$$

where $(\hat{\Theta}^{(G)}, \hat{\mathbb{U}}^{(G)}, \hat{\pi}^{(G)}) = \arg_{(\Theta, \mathbb{U}, \pi)} \max \ell_c^{(G)}(\Theta, \mathbb{U}, \pi)$, λ_{mT} is a reference tuning parameter sequence satisfying $\lambda_{mT}/mT \rightarrow 0$ and $\lambda_{mT}/(mTn_b^{-r}) \rightarrow \infty$. We then have

$$P\left(\min_{G' \neq G} LIC_{G'} < LIC_G\right) \rightarrow 1.$$

The proof of Theorem 4 is given in Appendix B.5. By Theorem 4, as long as the tuning parameter λ_{mT} is appropriately chosen, the true number of groups G could be consistently identified.

4. MODEL ESTIMATION USING StEM ALGORITHM

In this section, we discuss the numerical algorithm for model estimation. Although directly maximizing the constrained likelihood functions is straightforward, it is problematic mainly due to computational difficulties. According to Veen and Schoenberg (2008), due to the flatness and multimodal forms of the log-likelihood function, it might lead to highly unstable results and the final convergence heavily depends on initial value settings. Therefore they recommend using an EM-type algorithm for robust and accurate estimation.

In this work, we further revise the conventional EM-type algorithm to a stochastic version for the proposed NGH process. It is shown to have computational advantages, especially for complex Hawkes process models. The proposed algorithm is able to estimate the unknown parameters as well as latent group memberships simultaneously. To this end, a new branching structure is firstly introduced, and details of the StEM algorithm are then given in the following several sections.

4.1. The Branching Structure Representation of NGH Process

To introduce the StEM algorithm, we first present a branching structure of the NGH process. That enables us to view the NGH process as an incomplete data problem and thus the EM-type algorithm can be employed.

The branching structure representation of a traditional Hawkes process (2.1) is firstly introduced by Hawkes and Oakes (1974). They demonstrate that the events can be classified into two disjoint processes: a *background process* which is simply a Poisson process with rate ν , and *offspring processes* which are triggered by preceding events and the intensities are determined by $f(\cdot)$ in (2.1). In the context of earthquake analysis, for the i th event, an unobserved variable Z_i is introduced to denote whether it is generated by the background process or triggered by preceding events. Specifically, set $Z_i = 0$ if it is generated by the background process, and $Z_i = j$ if it is triggered by the previous j th earthquake. This leads to the branching structure of the univariate Hawkes process in the left panel of Figure 4. According to Hawkes and Oakes (1974), the resulting process of the branching structure is equivalent to the process generated by (2.1).

The branching structure of the NGH process model is more complicated, since the events can be triggered by both the nodes themselves and their friends. To state more clear, the posting event of the node i at time t can be generated by the following three components.

- **BASELINE COMPONENT:** $\mu_{g_i}(t)$. The events generated by the baseline component represent daily periodic behaviors of the network users.

- **MOMENTUM COMPONENT:** $\beta_{g_i} \sum_{t_{ik} < t} f(t - t_{ik}; \eta_{g_i})$. The momentum component could be treated as a self-exciting part, which is the same as in the original Hawkes process (Hawkes and Oakes, 1974).
- **NETWORK COMPONENT:** $\sum_{j=1}^m \alpha_{g_i g_j} w_{ij} \sum_{t_{jl} < t} f(t - t_{jl}; \gamma_{g_i})$. The network component takes account for the mutual interactions of previous events from the following friends.

As one can see, previous events from both user themselves (i.e., momentum component) and their connected friends (i.e., network component) are capable to elevate the likelihood of future events. We further illustrate the branching structure of the NGH process model using a network with two nodes in the right panel of Figure 4. Specifically, suppose Node 1 follows Node 2 in this two-node network. The blue circle represents the event generated by baseline intensity. Besides, the events of the Node 1 could not only be triggered by its own previous events (denoted by purple circles), but also by Node 2 (denoted by green circles).

With respect to the branching structure, a complete-data likelihood function will be firstly given and corresponding StEM algorithm is then presented for model estimation. We discuss the details in the following sections.

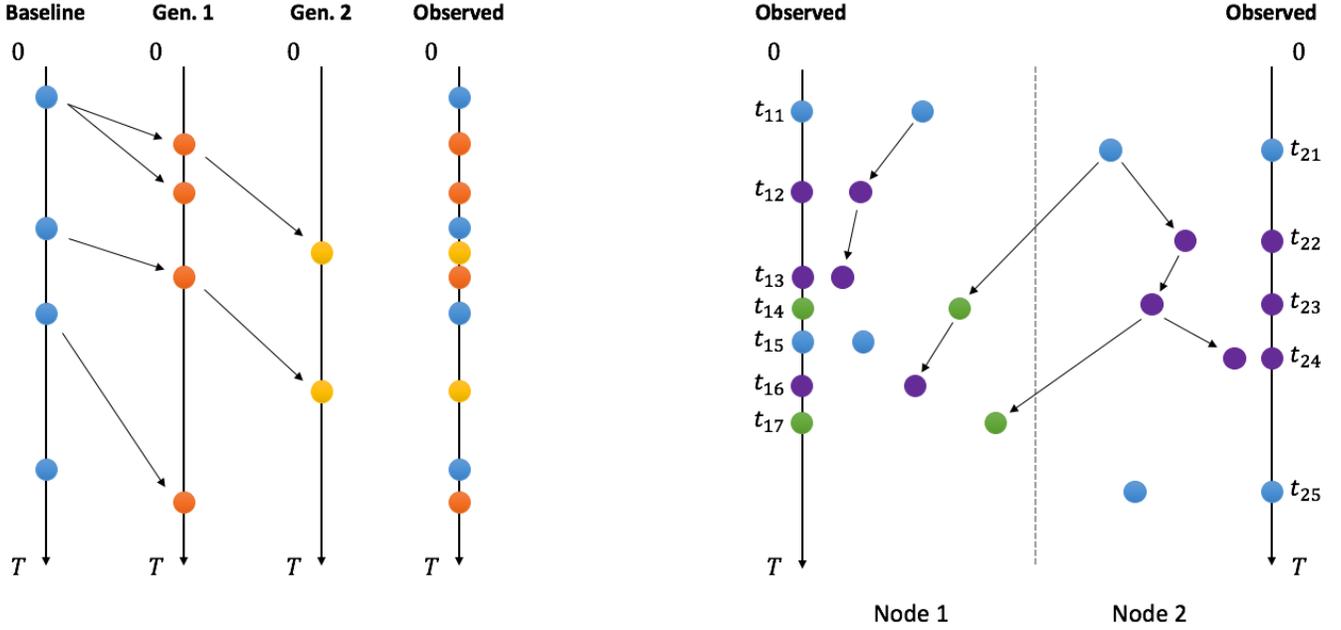


Figure 4: Branching Structure Representation of the classical Hawkes process (the left panel) and the NGH process (the right panel). The timeline goes from the top 0 to the bottom T . The left panel: the observed events are separated into baseline events and two generations of offspring events; The right panel: the event processes of two nodes within $[0, T]$ are presented, where Node 1 follows Node 2. The blue circle represents the event generated by baseline intensity, the purple circle indicates the event triggered by momentum component, the green circle is the event generated from network component.

4.2. Maximum Likelihood Estimation of the Branching NGH Process Model

In this section, we provide the maximum likelihood estimation for NGH process model with a branching structure. Following Hawkes (1971), we partition the events of the i th user into disjoint processes: a *background process*, which is a Poisson process with intensity $\mu_{g_i}(t)$, *momentum processes*, which origin from the user's own previous events with intensity $\beta_{g_i}f(t; \eta_{g_i})$, and the *network processes*, which origin from the historical events from following friends (i.e., $\{j : a_{ij} \neq 0\}$) with intensities $\alpha_{g_i g_j} d_i^{-1} f(t; \gamma_{g_i})$. Accordingly, for the k th event of the i th user, define a latent event type $Z_{ik} = (j, l)$, where $j = l = 0$ implies the k event is generated from the background process, and otherwise it means the k th event is triggered by the l th event from the j th user at a previous time point t_{jl} . Particularly, if $j = i$ then it indicates the current event is triggered by the users' own previous events, i.e., momentum components. For convenience, for the node i , define

$\lambda_i^{(i,k)}(t|\mathcal{G}) = \beta_{g_i} f(t - t_{ik}; \eta_{g_i})$ and $\lambda_i^{(j,l)}(t|\mathcal{G}) = \alpha_{g_i g_j} d_i^{-1} a_{ij} f(t - t_{jl}; \eta_{g_i})$ as intensity functions from momentum component and network component respectively. Then the complete-data likelihood function for the branching NGH process is given by

$$L_b(\theta) = \prod_{i=1}^m \prod_{g=1}^G \left[\pi_g \left\{ \prod_{k=1}^{n_i} \mu_i(t_{ik})^{I\{Z_{ik}=(0,0)\}} \prod_{j=1}^m \prod_{l=1}^{n_j} \lambda_i^{(j,l)}(t_{ik}|\mathcal{G})^{I\{Z_{ik}=(j,l)\}} \right\} S_i(T) \right]^{I\{g_i=g\}}, \quad (4.1)$$

where

$$S_i(T) = \prod_{j=1}^m \prod_{l=1}^{n_j} \exp \left\{ -\Lambda_i^{(j,l)}(T) \right\}, \quad \Lambda_i^{(j,l)}(T) = \int_0^T \lambda_i^{(j,l)}(t|\mathcal{G}) dt. \quad (4.2)$$

Here the complete-data likelihood function is different from (3.3) by further taking a latent event type Z_{ik} into consideration. The corresponding log-likelihood function is

$$\begin{aligned} \ell_b(\theta) = & \sum_{i=1}^m \sum_{g=1}^G I\{g_i = g\} \left[\log(\pi_g) \left\{ \sum_{k=1}^{n_i} I\{Z_{ik} = (0,0)\} \log \mu_i(t_{ik}) \right. \right. \\ & \left. \left. + \sum_{j=1}^m \sum_{l=1}^{n_j} I\{Z_{ik} = (j,l)\} \log \lambda_i^{(j,l)}(t_{ik}|\mathcal{G}) \right\} + \log S_i(T) \right]. \end{aligned} \quad (4.3)$$

To optimize the complete log-likelihood objective function (4.3), a conventional approach is to use an EM algorithm (Veen and Schoenberg, 2008; Halpin et al., 2013; Fox et al., 2016). However, this approach is computationally infeasible under our framework. The reason is as follows. In the E-step of the classical EM algorithm, to calculate the expectation of the log-likelihood, we need to obtain the joint posterior distribution of all latent variables. Denote $\mathcal{M}_i = \{\mu_{g_i}(t), \lambda_i^{(j,l)}(t) : j \in \{i\} \cup \{j' : a_{ij'} \neq 0\}, 1 \leq l \leq n_j\}$ as the set of intensity functions for the node i . It will include $G^N \times \prod_{i=1}^m |\mathcal{M}_i|^{n_i}$ combinations of latent variables to sum up in each iteration, which is computationally infeasible. As an alternative, the stochastic version of the EM algorithm only requires one sampling point of each latent variable in the E-step. In this regards, the StEM algorithm has competitive computational advantages, especially for our setting. The algorithm details are presented in the following section.

4.3. Stochastic EM Algorithm

The stochastic EM algorithm (Diebolt and Ip, 1995) could be divided into two steps, i.e., the stochastic E-step (StE-Step) and the M-step. In the StE-Step, we calculate the expectation of the log-likelihood (4.3) by deriving the posterior distribution of all latent variables. Next, in the M-step, we optimize the log-likelihood function (4.3) by using the sampling points from the StE-Step. We describe the two steps in details as follows.

Step I: Stochastic E-step

First, in the StE-step, we generate random samples from the posterior distribution of all latent variables. Specifically, they include the latent types of all events $\mathcal{Z} = \{Z_{ik} : 1 \leq i \leq m, 1 \leq k \leq n_i\}$, and the latent memberships $\mathcal{G} = \{g_i : 1 \leq i \leq m\}$. We first generate Z_{ik} from a categorical distribution with posterior probability

$$P\{Z_{ik} = (0, 0) | \mathcal{G}\} = \frac{\mu_i(t_{ik})}{\mu_i(t_{ik}) + \sum_{j=1}^m \sum_{l=1}^{n_j} \lambda_i^{(j,l)}(t_{ik} | \mathcal{G})}, \quad (4.4)$$

$$P\{Z_{ik} = (j, l) | \mathcal{G}\} = \frac{\lambda_i^{(j,l)}(t_{ik} | \mathcal{G})}{\mu_i(t_{ik}) + \sum_{j=1}^m \sum_{l=1}^{n_j} \lambda_i^{(j,l)}(t_{ik} | \mathcal{G})}, \quad \text{for } 1 \leq j \leq m, 1 \leq l \leq n_j. \quad (4.5)$$

Subsequently, we generate g_i from a posterior categorical distribution by

$$P(g_i = g | \mathcal{Z}) = \frac{\pi_g [\{\prod_{k=1}^{n_i} \tilde{f}_{ii}(t_{ik})\} \prod_{j \neq i} \{\prod_{k=1}^{n_i} \tilde{f}_{ij}(t_{ik})\} \{\prod_{l=1}^{n_j} \tilde{f}_{ji}(t_{jl})\} \tilde{S}_i(T)]^{I(g_i=g)}}{\sum_g \pi_g [\{\prod_{k=1}^{n_i} \tilde{f}_{ii}(t_{ik})\} \prod_{j \neq i} \{\prod_{k=1}^{n_i} \tilde{f}_{ij}(t_{ik})\} \{\prod_{l=1}^{n_j} \tilde{f}_{ji}(t_{jl})\} \tilde{S}_i(T)]^{I(g_i=g)}}, \quad (4.6)$$

where

$$\begin{aligned} \tilde{f}_{ij}(t_{ik}) &= \left\{ \mu_i(t_{ik})^{I\{Z_{ik}=(0,0)\}} \right\} \left\{ \prod_{l=1}^{n_j} \lambda_i^{(j,l)}(t_{ik} | \mathcal{G})^{I\{Z_{ik}=(j,l)\}} \right\}, \\ \tilde{S}_i(T) &= \left[\prod_{j=1}^m \prod_{l=1}^{n_j} \exp\{-\Lambda_i^{(j,l)}(T)\} \right] \left[\prod_{j \neq i} \prod_{k=1}^{n_i} \exp\{-\Lambda_j^{(i,k)}(T)\} \right], \end{aligned}$$

and $\Lambda_i^{(j,l)}(T)$ is defined in (4.2). To better understand the complicated forms of the posterior distributions of Z_{ik} and g_i , we give the following remark.

Remark 3. We first comment on the posterior distribution of the latent event types $\{Z_{ik} : 1 \leq i \leq m, 1 \leq k \leq n_i\}$. For the node i , each event type is generated by using (4.4)–(4.5) under the framework of the branching theory (Daley and Vere-Jones, 2003). Particularly, the occurrence probability of one event type will be proportional to the magnitude of the corresponding intensity. Next, given the generated latent event types, we could generate the latent memberships by using (4.6). Despite its complicated forms, we would like to remark that the posterior distribution of g_i for the node i mainly includes three parts. The first part is *self-exciting impact*, i.e., $\prod_{k=1}^{n_i} \tilde{f}_{ii}(t_{ik})$. This part refers to the influence of the nodes' own historical events. The second part is *in-going network impact*, i.e., $\prod_{j \neq i} \prod_{k=1}^{n_i} \tilde{f}_{ij}(t_{ik})$. Specifically, this part reflects the impact from the node i 's all following friends. Lastly, the third part, i.e., $\prod_{j \neq i} \prod_{l=1}^{n_i} \tilde{f}_{ji}(t_{jl})$, reflects the *out-going network impact*, which refers to the influence of the node i on its all connected followers. As a result, computationally, for single node i , only the intensities of its own and connected friends will be involved. This fact reduces the computational burden greatly, especially for a large scale sparse network.

After all the latent variables are generated, we are able to conduct parameter estimation in the M-step as follows.

Step II: M-step

In the M-step, we first update the baseline intensity function. Next, we estimate all parameters by maximizing the complete-data likelihood function under the branching structure. In the n th iteration, suppose we already generate samples $\{Z_{ik}^{(n)} : 1 \leq i \leq m, 1 \leq k \leq n_i\}$ and $\{g_i^{(n)} : 1 \leq i \leq m\}$ from the StE-step.

(A) UPDATE BASELINE INTENSITY FUNCTION.

To estimate the baseline intensity function, we set the basis function $k_j(t; h)$ in $\Phi_b = \{k_j(t; h), 1 \leq$

$j \leq n_b$ as $k_j(t; h) = h^{-1}K(h^{-1}(t - t_j))$, where $K(\cdot)$ is a standard Gaussian kernel function and h is a hyperparameter. Specifically, we set $n_b = 72$, $t_j = (j - 1)/3$, and the period $\omega = 24$ hours in our case. We then proceed to estimate the corresponding weights in (3.1). To this end, we first partition $[0, \omega]$ by $\{t_1, \dots, t_{n_b}\}$. Define $\mathcal{J}(t_{ik}) = [(t_{ik} \bmod \omega) \times 3] + 1$, where $[R]$ denotes the integer part of R . If $\mathcal{J}(t_{ik}) = j$, then t_{ik} should be counted into the interval $[t_j, t_{j+1}]$. Let $\mathcal{C}_j^{(g)} = \sum_{i=1}^m \sum_{k=1}^{n_i} I\{g_i = g, Z_{ik}^{(n)} = (0, 0), \mathcal{J}(t_{ik}) = j\}$ and $\bar{\mathcal{C}}^{(g)} = m_g^{-1} \sum_i \sum_k I\{g_i = g, Z_{ik}^{(n)} = (0, 0)\}$, where $m_g = \sum_g I(g_i = g)$. In addition, let $\mathcal{C}^{(g)} = \sum_j \mathcal{C}_j^{(g)} \int_0^T k_j(t; h) dt$. Then the weight $w_j^{(g)}$ for the g th group is estimated by $\hat{w}_j^{(g)} = \bar{\mathcal{C}}^{(g)} \mathcal{C}_j^{(g)} / \mathcal{C}^{(g)}$. Subsequently $\mu_g(t)$ is given by $\hat{\mu}_g^{(n)}(t) = \sum_{j=1}^{n_b} \hat{w}_j^{(g)} k_j(t; h)$. In practice, we choose h by data-driven method provided by Scott (2015) and also make it group-specific.

(B) UPDATE MODEL PARAMETER ESTIMATES.

After updating the baseline intensity function, we plug-in the generated samples into (4.3) and optimize the log-likelihood function (4.3) with respect to Θ . Here we follow Halpin et al. (2013) to set the triggering function $f(t; \gamma)$ in as $f(t; \gamma) = \gamma \exp(-\gamma t)$. This yields

$$\pi_g^{(n)} = \frac{\sum_{i=1}^m I\{g_i^{(n)} = g\}}{m}, \quad (4.7)$$

$$\beta_g^{(n)} = \frac{\sum_{i=1}^m \sum_{k,l=1}^{n_i} I\{g_i^{(n)} = g, Z_{ik}^{(n)} = (i, l)\}}{\sum_{i=1}^m \sum_{k=1}^{n_i} I\{g_i^{(n)} = g\} [1 - \exp\{-\eta_g^{(n)}(T - t_{ik})\}]}, \quad (4.8)$$

$$\eta_g^{(n)} = \frac{\sum_{i=1}^m \sum_{k,l=1}^{n_i} I\{g_i^{(n)} = g, Z_{ik}^{(n)} = (i, l)\}}{\sum_{i=1}^m I\{g_i^{(n)} = g\} \sum_{l=1}^{n_i} \Delta_{1,il}(\beta_g^{(n)}, \eta_g^{(n)}, T)}, \quad (4.9)$$

$$\alpha_{g_1 g_2}^{(n)} = \frac{\sum_{i,j=1}^m \sum_{k=1}^{n_i} \sum_{l=1}^{n_j} I\{g_i^{(n)} = g_1, g_j^{(n)} = g_2, Z_{ik}^{(n)} = (j, l)\}}{\sum_{i,j=1}^m \sum_{l=1}^{n_j} I\{g_i^{(n)} = g_1, g_j^{(n)} = g_2\} \cdot \omega_{ij} [1 - \exp\{-\gamma_{g_1}^{(n)}(T - t_{jl})\}]}, \quad (4.10)$$

$$\gamma_g^{(n)} = \frac{\sum_{i,j=1}^m \sum_{l=1}^{n_j} \sum_{k=1}^{n_i} I\{g_i^{(n)} = g, Z_{ik}^{(n)} = (j, l)\}}{\sum_{i=1}^m I\{g_i^{(n)} = g\} \sum_{j=1}^m \sum_{l=1}^{n_j} \Delta_{2,ijl}(\alpha_{gg_j}^{(n)}, \gamma_g^{(n)}, T)} \quad (4.11)$$

where

$$\begin{aligned}\Delta_{1,il}(\beta_g^{(n)}, \eta_g^{(n)}, T) &= \sum_{k=1}^{n_i} I\{Z_{ik}^{(n)} = (i, l)\}(t_{ik} - t_{il}) + \beta_g^{(n)}(T - t_{il})\exp\{-\eta_g^{(n)}(T - t_{il})\}, \\ \Delta_{2,ijl}(\alpha_{gg_j}^{(n)}, \gamma_g^{(n)}, T) &= \sum_{k=1}^{n_i} I\{Z_{ik}^{(n)} = (j, l)\}(t_{ik} - t_{jl}) + \alpha_{gg_j}^{(n)}\omega_{ij}(T - t_{jl})\exp\{-\gamma_g^{(n-1)}(T - t_{jl})\}.\end{aligned}$$

Let $\Theta^{(n)}$ be the estimator obtained from the n th iteration. We obtain the final estimator $\hat{\Theta}$ by dropping the first L burn-in samples and taking average of the subsequent R samples as

$$\hat{\Theta} = \frac{1}{R} \sum_{n=L+1}^{L+R} \Theta^{(n)}. \quad (4.12)$$

The detailed procedure to determine L and R are provided in Appendix D.1. We summarize the StEM algorithm in Algorithm 1.

Algorithm 1: StEM Algorithm for NGH Process Model.

0. Initial : Initial estimator $\Theta^{(0)}$, initial membership $\{g_i^{(0)}\}_{i=1}^m$.

For $n = 1, 2, \dots$, **repeat Steps 1–3 as follows**

1. StE-step:

- 1) Sample $Z_{ik}^{(n)}$ using the Categorical distribution with probability (4.4) and (4.5) for $1 \leq i \leq m, 1 \leq k \leq n_i$.
- 2) Sample $g_i^{(n)}$ from the Categorical distribution with probability (4.6) for $1 \leq i \leq m$.

2. M-step :

- 1) Obtain the estimated baseline intensity $\hat{\mu}_g^{(n)}(t)$.
- 2) Update the parameters $\Theta^{(n)}$ by (4.7)–(4.11).

3. Output : Determine whether the burn-in stage is over by Algorithm 2 in Appendix C.2. If it is over, then determine R by Algorithm 3 in Appendix C.2 and output the final estimator $\hat{\Theta}$ by (4.12).

5. SIMULATION STUDIES

5.1. Simulation Models

In this section, we present a number of simulation studies to gauge the numerical performance of the proposed method. The main differences lie in the generating mechanism of group settings as well as the network structures. Across all settings, we consider a periodic function to mimic the daily activities of the network users as follows

$$u(t) = h_1 + h_2 \sum_{k=0}^H I(t \in [k\omega_0 - \omega_1, k\omega_0 + \omega_1]).$$

In the formulation of $u(t)$, h_1 is a constant representing a baseline activity level. In addition, in every ω_0 hours, users increase their activity levels by an extra amount of h_2 , which lasts for $2\omega_1$ hours. During this period, the users are more likely to be active on social networks. We set $\omega_1 = 0.04$ hours (i.e., 2.5 minutes) for all groups and consider various activity levels (i.e., h_1 and h_2) and periodic parameters (i.e., ω_0) for different groups.

Next, we specify the number of groups as $G = 3$ with unbalanced group size as $\pi = (0.2, 0.5, 0.3)^\top$. Subsequently, we set $h_1 = (0.75, 0.50, 0.25)$ and $h_2 = (6.75, 4.50, 2.25)$ in the baseline function to represent different activity levels. In addition, the periodic parameters are set to be $\omega_0 = 3, 6, 12$ hours respectively. Next, the parameters in the momentum intensities are set to be $(\beta_1, \beta_2, \beta_3) = (0.5, 0.4, 0.7)$ and $(\eta_1, \eta_2, \eta_3) = (1.5, 1, 2)$. As a result, the last group is more self-excited than the other two groups. Lastly, the parameters in the network intensity are set to be $(\gamma_1, \gamma_2, \gamma_3) = (1, 2, 0.5)$ and $\alpha = (0.4, 0.1, 0.1; 0.6, 0.4, 0.5; 0.15, 0.2, 0.1) \in \mathbb{R}^{3 \times 3}$. Consequently, compared to the other two groups, the last group is less influenced and more self-motivated. We consider the following two typical network structures in our simulation study.

NETWORK STRUCTURE I: POWER-LAW DISTRIBUTION NETWORK. In a power-law network (Barabási and Albert, 1999), only a few nodes have large numbers of edges, while most of nodes possess few edges. The adjacency matrix A under this assumption could be simulated in the following steps. For each node i , we first generate the in-degree $d_i = \sum_{j=1}^m a_{ji}$ by sampling from a power-law distribution, i.e., $P(d_i = d) = cd^{-\alpha}, 0 \leq d \leq m$, where c is a normalizing constant and α is set to be $\alpha = 2.4$. Then we randomly pick d_i nodes (except the i th node itself) as its followers.

By doing the two steps for $i = 1, \dots, m$, we can generate a power-law distribution network.

NETWORK STRUCTURE II: STOCHASTIC BLOCK MODEL. The stochastic block model (Wang and Wong, 1987) is widely considered in community detection problems (Karrer and Newman, 2011). To generate this type of network, we first randomly assign the block labels b_i for each node i with equal probabilities, where $b_i = 1, \dots, B$ with $B = 3$. Once the blocks are determined, we generate the edges with probability $P(a_{ij} = 1) = 0.3m^{-0.3}$ if they belong to the same block (i.e., $b_i = b_j$), and $P(a_{ij} = 1) = 0.3m^{-1}$ otherwise. As a result, the nodes are more likely to be connected within the same blocks.

Given the above simulation settings, we could then generate the events for all network users by using the branching structure of the NGH process model. The generating procedure is described in Algorithm 4 and 5 in Appendix D.2 in the supplementary material.

5.2. Performance Measurements and Simulation Results

Different sample sizes are considered to evaluate the finite sample performance. Specifically, we set $\{m = 1000, T = 48h\}$ and $\{m = 1500, T = 72h\}$ to verify the estimation properties. For a reliable evaluation, we randomly repeat the experiment for $R = 100$ times.

Denote $\hat{\Theta}^{(r)} = (\hat{\Theta}_j^{(r)})^\top$ as the parameter estimates obtained in the r th replication. We first measure the parameter estimation accuracy. To this end, the root mean square error for each parameter is calculated as $\text{RMSE}_j = \{R^{-1} \sum_{r=1}^R (\hat{\Theta}_j^{(r)} - \Theta_j)\}^{1/2}$. Next, we evaluate the group estimation accuracy. Denote $\hat{g}_i^{(r)}$ as the estimated group label for the i th node after conducting group permutation in the r th simulation. We then calculate the group estimation accuracy (GAE) as $\text{GAE}^{(r)} = m^{-1} \sum_{i=1}^m I(\hat{g}_i^{(r)} = g_i)$ and the average GAE is reported.

The simulation results are presented in Table 1. First, as the sample size increases, the parameter estimations tend to be more accurate. For instance, as $\{m, T\}$ increases from $\{1000, 48h\}$ to $\{1500, 72h\}$, the RMSE of β decreases from 6.60×10^{-3} to 5.60×10^{-3} for Group 1 of under POWER-LAW DISTRIBUTION NETWORK. This corroborates with the theoretical result in Theorem

1. Similarly, we are able to achieve a relatively higher group estimation accuracy with larger sample sizes. This further confirms our theoretical findings in Theorem 3.

6. EMPIRICAL STUDY: A SINA WEIBO DATASET

6.1. Data Description

In this section, we conduct an empirical study using a Sina Weibo dataset to illustrate the usefulness of the proposed NGH process model. The dataset is collected from Sina Weibo (*www.weibo.com*) platform, which is the largest Twitter type online social media in mainland China. Specifically, we collect the posting behaviors of $m = 2,038$ users from January 1st to January 15th, 2014. For each user i , we could observe a sequence of his/her Weibo posting time stamps $\{t_{i1}, \dots, t_{in_i}\}$. We give an example of two Weibo posts by James Cameron in Figure 5, where the corresponding posting times are highlighted by red rectangles.



Figure 5: The Sina Weibo data analysis. A snapshot of James Cameron’s Weibo posts. The corresponding posting times are highlighted by red rectangles.

The adjacency matrix A is constructed by the following-follower relationship among the users, where the network density is $\sum_{i,j} a_{ij}/m(m-1) = 2.7\%$. This indicates a high sparsity level. We further present the histograms of in-degrees and out-degrees in Figure 6. It can be observed that the distribution of in-degrees is more skewed than the out-degrees. This implies the existence of “superstars” in the network.

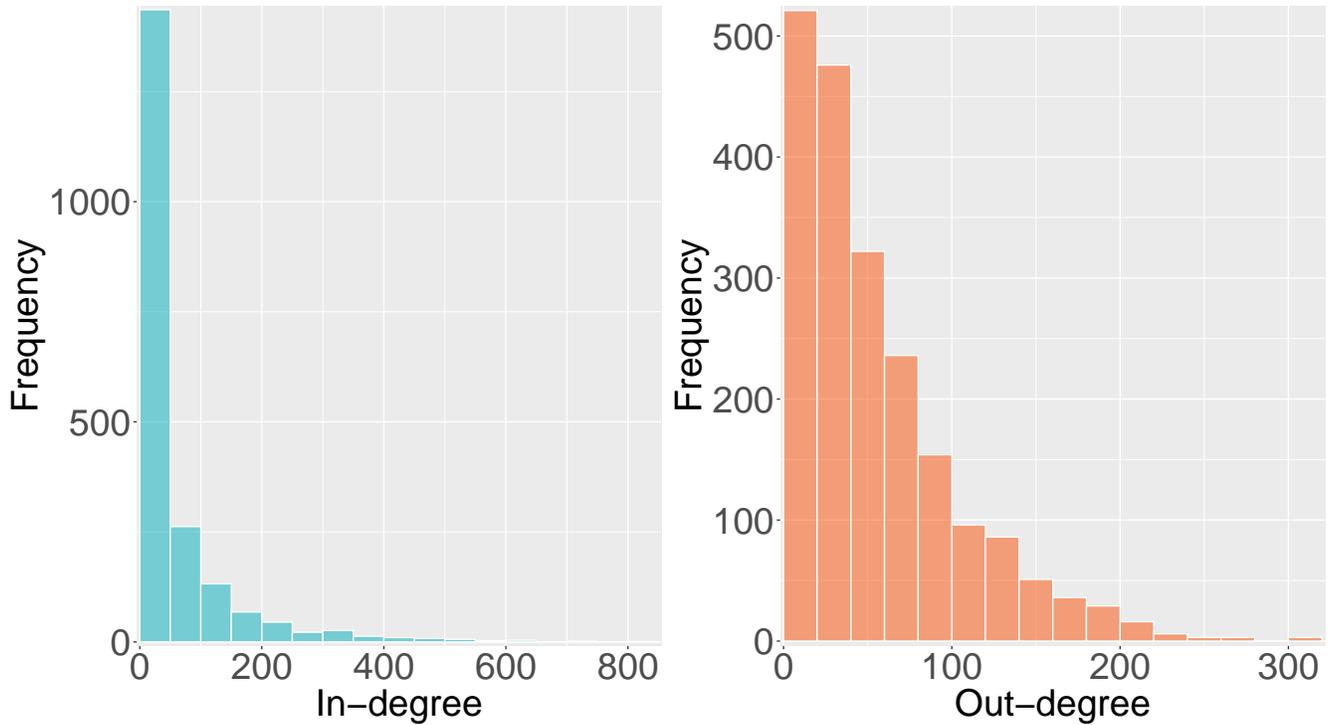


Figure 6: The Sina Weibo data analysis. The left panel: histogram of in-degrees for $m = 2038$ nodes; the right panel: histogram for out-degrees.

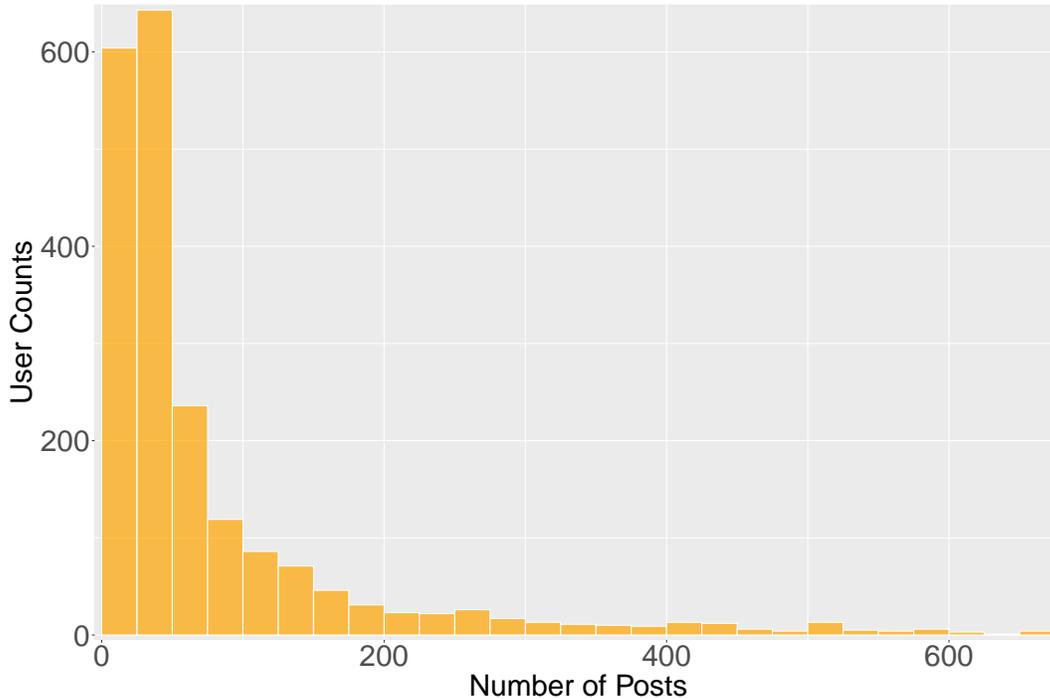


Figure 7: The histogram of total number of posts for $m = 2038$ users in the Sina Weibo dataset.

Next, we conduct a descriptive analysis of the user posting behaviors. First, for each user, we calculate his/her number of posts for 15 days. This yields the histogram in Figure 7. The median value is given by 39, which indicates that the users have 2.6 posts per day on an average level. Next, to show the dynamic patterns of the user posting behaviors, we calculate the aggregated number of posts for all users within every 6 hours. This leads to the barplot in Figure 3. A clear periodic pattern can be observed. In addition, we find that most Weibo posts are posted from 6:00 am to 6:00 pm.

6.2. Model Estimation and Interpretation

Motivated by the preliminary analysis, we conduct model estimation using the proposed StEM algorithm. First, we select $G = 6$ according to the criterion in (3.10). For each group, the estimated baseline intensity functions are drawn in Figure 8. Despite the differences, we could observe that most groups have higher intensity levels during 9:00 am to 9:00 pm. Next, the parameter estimation

results are given in Table 2. The standard errors are obtained using a parametric bootstrap method (Efron, 1982). To further show the influencing patterns among different groups, we visualize the estimated group network coefficient $\hat{\alpha}$ in Figure 9. In the following, we describe the characteristics of each group as well as their dynamic patterns.

- Group 1. (CELEBRITY GROUP) Most group members in this group are famous celebrities who have a large number of followers. According to the baseline intensity estimation in Figure 8, the users in this group tend to post less frequently than the other groups. However, it can be observed from Figure 9 that this group has relatively stronger influences on the others.
- Group 2. (FINANCE GROUP) This group includes mostly financial news accounts. As shown in Figure 8, users in this group are the most active during the morning periods from 8:00 am to 11:00 am.
- Group 3. (SCHOLAR GROUP) This group consists mostly of scholars with backgrounds in economics and social science. The users in this group are more active around 10:00 am and 10:00 pm. Indicated by the parameter estimation result (i.e., Table 2 and Figure 9), this group is more self-driven (i.e., higher β_g) than influenced by others.
- Group 4. (PUBLIC ACCOUNT) This group consists mostly of public accounts, who release daily news information. From Figure 8, this group has the highest activity levels among all groups. Compared to other groups, the users in this group post more frequently in the afternoon and evening. In addition, this group is also found to be more self-driven in their posting behaviors.
- Group 5. (STRONG-CONNECTED GROUP) This group is characterized by the highest group network coefficient $\hat{\alpha}_{gg}$ in Figure 9. As a result, the users in this group are strongly affected by their connected friends within the same group. We find many strongly related accounts in this group, such as “Fudan University” and “School of Management of Fudan University”.

- Group 6. (ORDINARY GROUP) The rest of the network users are classified as the “ordinary group”. Compared to the other groups, this group has limited influential powers but is more likely to be influenced by the others.

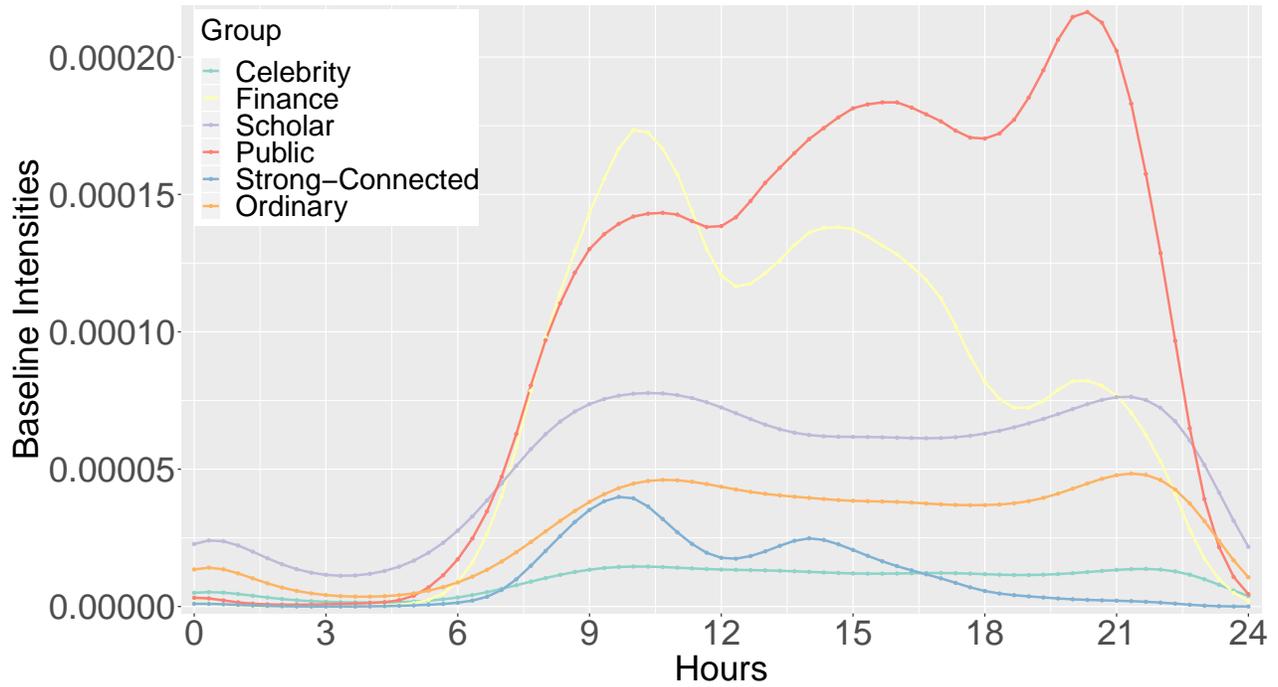


Figure 8: The estimated baseline intensities for each group in the Sina Weibo data analysis.



Figure 9: The heatmap of estimated α in the Sina Weibo data analysis.

6.3. Influential User Analysis

In social network analysis, identifying influential users are critically important for online social platforms. It could help to spread news efficiently, release products, as well as launch promotion campaigns (Aral and Walker, 2011; Stephen and Galak, 2012; Zhu et al., 2019). In this section, we conduct influential power analysis for network users based on the branching structure of the NGH process model.

In the branching structure of the NGH process model, recall that the latent event type $Z_{jl} = (i, k)$ represents that the event $\{t_{jl}\}$ of the user j is triggered by the event $\{t_{ik}\}$ of the user i . Consequently, if the user i is an influential user, he/she will have enough powers to trigger as many subsequent events as possible on its followers. Specifically, for each event $\{t_{ik}\}$ of the user i , we are able to calculate the number of its triggering events from other users, i.e., $\nu_{ik} \stackrel{\text{def}}{=} \sum_{j \neq i} \sum_{l=1}^{n_j} I\{Z_{jl} =$

(i, k) . We then refer to ν_{ik} as the *influential effect* of the event $\{t_{ik}\}$. As a result, the *influential power* of the user i can be naturally defined by aggregating the influential effects of all events for the user i , i.e.,

$$\text{infl}_i = \sum_{k=1}^{n_i} \nu_{ik} = \sum_{k=1}^{n_i} \sum_{j \neq i} \sum_{l=1}^{n_j} I\{Z_{jl} = (i, k)\}. \quad (6.1)$$

We calculate the influential powers for all network users by using (6.1) with the estimated latent event types Z_{jl} . The top 10 users with the highest influential powers are visualized in Figure 10. It is found that these influential users are mainly online public media accounts, who behave actively on this online social platform to release daily financial and business news.

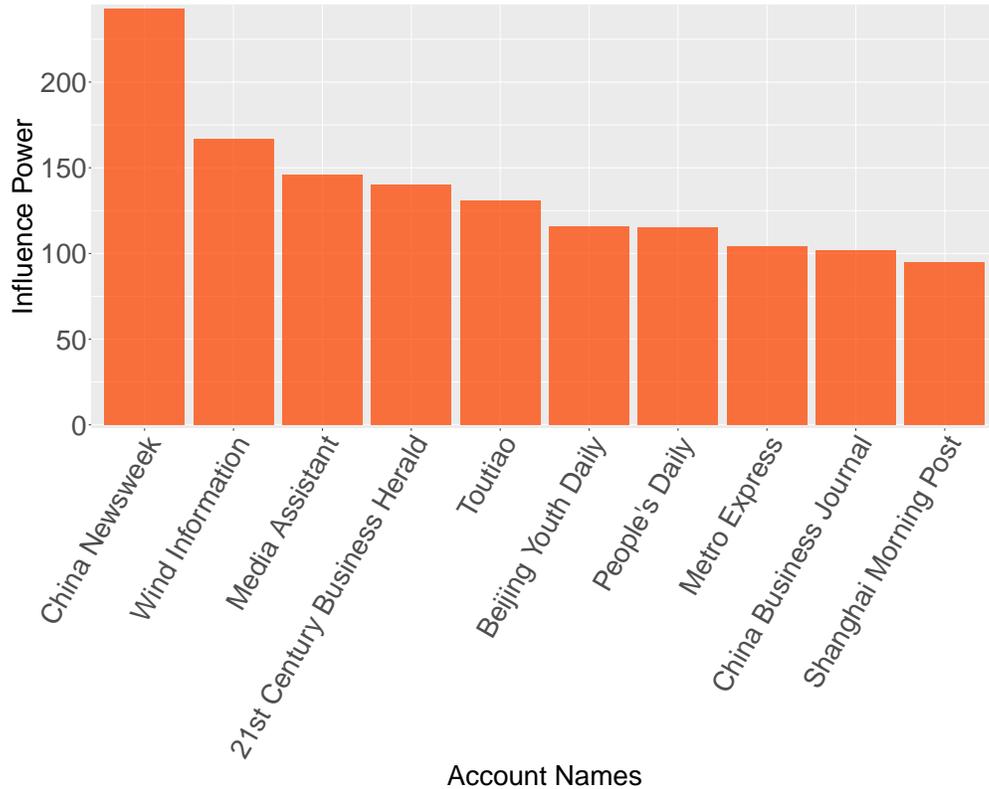


Figure 10: Sina Weibo Data Analysis: Barplot of the top 10 influential Weibo accounts. Most of the influential network users are online public media accounts who release financial and business news.

7. DISCUSSION

In this paper, we propose a network group Hawkes (NGH) process model to analyze the dynamic

behavior patterns of network users. The proposed model extends the classical Hawkes model by taking accounts of the observed network structure. In addition, the users are assumed to have latent groups according to their dynamic behavior patterns. The theoretical properties of parameter estimates including the consistency, asymptotic normality, and the identifiability of group memberships are established under certain conditions. Numerically, a StEM algorithm is designed to estimate the model based on a novel branching representation of the NGH process. Lastly, we apply the proposed model to a Sina Weibo dataset and obtain highly interpretable estimation results. As an interesting application, we further discuss the influential powers of the network users based on the model output. We would like to remark that the proposed method could be applied in abundant scenarios such as epidemic study, crime pattern analysis, consumer profile analysis, and many others, as long as the corresponding network structure can be defined.

To conclude the article, we provide several topics for future study. First, the NGH process model can be further extended by including covariates such as gender, region, user self-defined labels, longitudinal information (Blei et al., 2003; Shen et al., 2016; Xu et al., 2019). Next, only one type of user behaviors is taken into consideration. It is interesting to extend the model by incorporating multi-types of user behaviors. Third, the network structure in the current framework is assumed to be known and unchanged. Therefore, how to model dynamic relationships is an important problem for further investigation.

References

- Aral, S. and Walker, D. (2011), “Creating social contagion through viral product design: A randomized trial of peer influence in networks,” *Management Science*, 57, 1623–1639.
- Barabási, A.-L. and Albert, R. (1999), “Emergence of scaling in random networks,” *Science*, 286, 509–512.
- Blei, D. M., Ng, A. Y., and Jordan, M. I. (2003), “Latent dirichlet allocation,” *Journal of Machine*

Learning Research, 3, 993–1022.

Chen, S., Shojaie, A., Shea-Brown, E., and Witten, D. (2017), “The multivariate Hawkes process in high dimensions: Beyond mutual excitation,” *arXiv preprint arXiv:1707.04928*.

Cho, E., Myers, S. A., and Leskovec, J. (2011), “Friendship and mobility: user movement in location-based social networks,” in *Proceedings of the 17th ACM SIGKDD international conference on Knowledge discovery and data mining*, ACM, pp. 1082–1090.

Daley, D. and Vere-Jones, D. (2003), *An introduction to the theory of point processes: elementary theory and methods*, vol. I, New York: Springer.

Diebolt, J. and Ip, E. H. S. (1995), “A Stochastic EM algorithm for approximating the maximum likelihood estimate,” *Unpublished doctoral dissertation, Department of Statistics, Stanford University*.

Efron, B. (1982), *The jackknife, the bootstrap, and other resampling plans*, vol. 38, Siam.

Fan, J., Huang, T., and Li, R. (2007), “Analysis of longitudinal data with semiparametric estimation of covariance function,” *Journal of the American Statistical Association*, 102, 632–641.

Fan, J. and Li, R. (2001), “Variable selection via nonconcave penalized likelihood and its oracle properties,” *Journal of the American Statistical Association*, 96, 1348–1360.

Fox, E. W., Short, M. B., Schoenberg, F. P., Coronges, K. D., and Bertozzi, A. L. (2016), “Modeling E-mail Networks and Inferring Leadership Using Self-Exciting Point Processes,” *Journal of the American Statistical Association*, 111, 0–0.

Gao, X. and Zhu, L. (2018), “Functional central limit theorems for stationary Hawkes processes and application to infinite-server queues,” *Queueing Systems*, 90, 161–206.

Halpin, Peter, F., Boeck, D., and Paul (2013), “Modelling Dyadic Interaction with Hawkes Processes,” *Psychometrika*, 78, 793–814.

- Hawkes, A. G. (1971), “Spectra of some self-exciting and mutually exciting point processes,” *Biometrika*, 58, 83–90.
- Hawkes, A. G. and Oakes, D. (1974), “A Cluster Process Representation of a Self-Exciting Process,” *Journal of Applied Probability*, 11, 493–503.
- He, X. and Shi, P. (1996), “Bivariate tensor-product B-splines in a partly linear model,” *Journal of Multivariate Analysis*, 58, 162–181.
- Karrer, B. and Newman, M. E. (2011), “Stochastic blockmodels and community structure in networks,” *Physical Review E*, 83, 016107.
- Lehmann, E. L. and Casella, G. (2006), *Theory of point estimation*, Springer Science & Business Media.
- Liu, X., He, Q., Tian, Y., Lee, W.-C., McPherson, J., and Han, J. (2012), “Event-based social networks: linking the online and offline social worlds,” in *Proceedings of the 18th ACM SIGKDD international conference on Knowledge discovery and data mining*, ACM, pp. 1032–1040.
- Masuda, N., Takaguchi, T., Sato, N., and Yano, K. (2013), “Self-exciting point process modeling of conversation event sequences,” in *Temporal Networks*, Springer, pp. 245–264.
- Mohler, G. O., Short, M. B., Brantingham, P. J., Schoenberg, F. P., and Tita, G. E. (2011), “Self-exciting point process modeling of crime,” *Journal of the American Statistical Association*, 106, 100–108.
- Sayyadi, H., Hurst, M., and Maykov, A. (2009), “Event detection and tracking in social streams,” in *Third International AAAI Conference on Weblogs and Social Media*.
- Scott, D. W. (2015), *Multivariate density estimation: theory, practice, and visualization*, John Wiley & Sons.

- Shen, Y., Huang, H., and Guan, Y. (2016), “A conditional estimating equation approach for recurrent event data with additional longitudinal information,” *Statistics in Medicine*, 35, 4306–4319.
- Sit, T., Ying, Z., and Yu, Y. (2018), “Event History Analysis of Dynamic Communication Networks,” *arXiv preprint arXiv:1810.03296*.
- Srijith, P., Lukasik, M., Bontcheva, K., and Cohn, T. (2017), “Longitudinal modeling of social media with Hawkes process based on users and networks,” in *Proceedings of the 2017 IEEE/ACM International Conference on Advances in Social Networks Analysis and Mining 2017*, ACM, pp. 195–202.
- Stephen, A. T. and Galak, J. (2012), “The effects of traditional and social earned media on sales: A study of a microlending marketplace,” *Journal of Marketing Research*, 49, 624–639.
- Van der Vaart, A. W. (2000), *Asymptotic statistics*, vol. 3, Cambridge university press.
- Veen, A. and Schoenberg, F. P. (2008), “Estimation of Space-Time Branching Process Models in Seismology Using an Em-Type Algorithm,” *Journal of the American Statistical Association*, 103, 614–624.
- Wang, Y. J. and Wong, G. Y. (1987), “Stochastic blockmodels for directed graphs,” *Journal of the American Statistical Association*, 82, 8–19.
- Wang, Y. R., Bickel, P. J., et al. (2017), “Likelihood-based model selection for stochastic block models,” *The Annals of Statistics*, 45, 500–528.
- Xu, H., Fang, G., and Ying, Z. (2019), “A Latent Topic Model with Markovian Transition for Process Data,” *arXiv preprint arXiv:1911.01583*.
- Zhao, Y., Levina, E., Zhu, J., et al. (2012), “Consistency of community detection in networks under degree-corrected stochastic block models,” *The Annals of Statistics*, 40, 2266–2292.

Zhu, X., Chang, X., Li, R., and Wang, H. (2019), “Portal nodes screening for large scale social networks,” *Journal of Econometrics*, 209, 145–157.

Zhu, X., Pan, R., Li, G., Liu, Y., and Wang, H. (2017), “Network Vector Autoregression,” *The Annals of Statistics*, 45, 1096–1123.

Table 1: Simulation results with 100 replications. The average parameter estimation as well as RMSE values (given in parentheses) are reported. The group estimation accuracy (GAE, given in %) is also reported in each setting.

m	T	K	Group	π ($\times 10^{-2}$)	ν ($\times 10^{-1}$)	β ($\times 10^{-3}$)	η ($\times 10^{-3}$)	γ ($\times 10^{-2}$)	$\alpha(\times 10^{-1})$ ($\times 10^{-2}$)	GAE		
Power-Law Model												
1000	48h	3	1	0.17	30.25	0.50	1.51	1.01	4.08	1.27	95.23%	
				(1.48)	(4.72)	(6.60)	(22.7)	(4.05)	(3.67)	(3.50)		(2.44)
			2	0.52	20.37	0.41	1.02	1.99	5.89	4.23		4.91
				(1.75)	(2.55)	(4.81)	(13.1)	(3.08)	(2.58)	(2.78)		(1.57)
			3	0.31	10.19	0.70	1.99	0.50	1.51	1.89		1.07
				(1.41)	(2.37)	(7.34)	(24.2)	(1.23)	(1.10)	(1.35)		(1.19)
1500	72h	3	1	0.17	30.22	0.50	1.51	1.01	3.98	1.27	95.65%	
				(1.08)	(3.90)	(5.60)	(20.3)	(2.79)	(2.35)	(3.27)		(2.16)
			2	0.52	20.37	0.41	1.03	1.98	5.88	4.26		4.92
				(1.51)	(2.00)	(3.54)	(11.3)	(2.73)	(1.99)	(3.01)		(1.36)
			3	0.30	10.15	0.70	1.99	0.50	1.51	1.87		1.06
				(1.13)	(2.03)	(5.46)	(18.5)	(1.11)	(0.84)	(1.63)		(0.97)
Stochastic Block Model												
1000	48h	3	1	0.19	29.82	0.50	1.51	1.02	4.06	1.09	98.30%	
				(1.27)	(4.67)	(5.50)	(18.8)	(2.92)	(1.45)	(1.05)		(1.33)
			2	0.51	20.02	0.40	1.00	2.01	5.97	4.00		4.99
				(1.75)	(2.04)	(2.77)	(8.85)	(1.66)	(1.05)	(0.41)		(0.66)
			3	0.31	10.30	0.70	1.98	0.50	1.57	1.99		1.03
				(1.59)	(2.86)	(5.77)	(21.3)	(1.08)	(0.96)	(0.39)		(0.54)
1500	72h	3	1	0.19	29.77	0.50	1.50	1.05	4.08	1.08	98.68%	
				(1.08)	(3.27)	(4.78)	(14.3)	(2.04)	(1.34)	(0.90)		(1.06)
			2	0.51	19.92	0.40	1.01	2.01	5.99	4.01		4.98
				(1.43)	(1.78)	(2.35)	(6.68)	(1.25)	(0.67)	(0.35)		(0.57)
			3	0.31	10.35	0.70	1.99	0.51	1.55	1.98		1.02
				(1.18)	(2.31)	(4.34)	(16.8)	(0.96)	(0.67)	(0.32)		(0.39)

Table 2: Estimation results of the NGH process model with the Sina Weibo dataset. The standard errors of parameter estimates are provided in parentheses.

Group	CELEBRITY	FINANCE	SCHOLAR	PUBLIC ACCOUNT	STRONG- CONNECTED	ORDINARY
$\hat{\pi}$	0.46	0.08	0.08	0.06	0.09	0.24
($\times 10^{-4}$)	(10.5)	(1.77)	(3.18)	(1.72)	(10.1)	(4.75)
$\hat{\beta}$	0.37	0.31	0.60	0.62	0.39	0.32
($\times 10^{-3}$)	(3.85)	(6.73)	(4.93)	(4.79)	(10.3)	(4.60)
$\hat{\eta}(\times 10^{-3})$	2.85	0.213	2.14	0.329	0.236	0.520
($\times 10^{-6}$)	(36.6)	(3.98)	(25.2)	(3.40)	(6.81)	(10.2)
$\hat{\gamma}(\times 10^{-3})$	0.316	23.6	181	157	0.429	163
($\times 10^{-3}$)	(0.008)	(1.72)	(138)	(7.00)	(0.034)	(109)

APPENDIX A

Appendix A.1: Definitions and Assumptions for Theoretical Results

Definition 1. Let $\Phi_b = \{k_j(t) : 1 \leq j \leq n_b, t \in \mathbb{R}\}$ be a set of basis functions and $\ell(\cdot)$ be a twice-differentiable function. Define the derivative of $\ell(f(t))$ with respect to $f(t)$ given Φ_b as

$$\frac{\partial \ell(f(t))}{\partial f} = \left(\dot{\ell}(f(t))k_1(t), \dots, \dot{\ell}(f(t))k_{n_b}(t) \right)^\top, \quad (\text{A.1})$$

where $\dot{\ell}(\cdot)$ is the first order derivative of $\ell(\cdot)$.

Definition 2. Let $\ell(x)$ ($x \in \mathbb{R}$) and $f(t)$ ($t \in [0, T]$) be arbitrary two continuous functions. The function $\ell(f(t))$ is said to be continuous with respect to $f(t)$, if for any $\epsilon > 0$, there exists a $\delta > 0$, for all $\tilde{f}(t)$ satisfying $\|\tilde{f}(t) - f(t)\|_\infty < \delta$ it holds

$$\|\ell(\tilde{f}(t)) - \ell(f(t))\|_\infty < \epsilon.$$

(C5.a) Let $\lambda_{i,0}(t) = C_0 + C_0^2 \sum_{t_{ik} < t} \phi_c(t - t_{ik}) + C_0^2 \sum_{t_{jl} < t} a_{ij}/d_i \phi_c(t_{jl})$, where $\phi_c(s) = \exp(-cs)$ and

c is constant such that $0 < c < 2^{-1} \min\{\gamma_g^*, \eta_g^*, 1 \leq g \leq G\}$. Define

$$\Phi(\Theta) = \frac{1}{mT} \sum_i \int_0^T \frac{1}{\lambda_{i,0}(t)} \tilde{\lambda}_i(t; \Theta) \tilde{\lambda}_i(t; \Theta)^\top dt, \quad (\text{A.2})$$

where $\tilde{\lambda}_i(t; \Theta) \stackrel{\text{def}}{=} (\partial \lambda_i(t | \mathcal{G}^*) / \partial \Theta^\top, \mathbf{e}_{g_i}^\top \otimes \mathbf{k}(t)^\top)^\top \in \mathbb{R}^{q+Gn_b}$, $\mathbf{k}(t) = (k_1(t), k_2(t), \dots, k_{n_b}(t))^\top \in \mathbb{R}^{n_b}$. Write $\Phi(\Theta) = (\Phi_{11}(\Theta), \Phi_{12}(\Theta); \Phi_{21}(\Theta), \Phi_{22}(\Theta))$, where $\Phi_{11}(\Theta) \in \mathbb{R}^{q \times q}$, $\Phi_{12}(\Theta) \in \mathbb{R}^{q \times Gn_b}$, $\Phi_{21}(\Theta) \in \mathbb{R}^{Gn_b \times q}$, and $\Phi_{22}(\Theta) \in \mathbb{R}^{Gn_b \times Gn_b}$. Define $\tilde{\Phi}_1(\Theta) = \bar{\Phi}_{11}(\Theta) - \bar{\Phi}_{12}(\Theta) \{\bar{\Phi}_{22}(\Theta)\}^{-1} \bar{\Phi}_{21}(\Theta)$ and $\tilde{\Phi}_2(\Theta) = \bar{\Phi}_{22}(\Theta) - \bar{\Phi}_{21}(\Theta) \{\bar{\Phi}_{11}(\Theta)\}^{-1} \bar{\Phi}_{12}(\Theta)$, where $\bar{\Phi}_{k_1 k_2}(\Theta) \stackrel{\text{def}}{=} E\{\Phi_{k_1 k_2}(\Theta)\}$. Assume $\lim_{m, T \rightarrow \infty} \tilde{\Phi}_1(\Theta)$ and $\sigma_2(\Theta) \stackrel{\text{def}}{=} \lim_{m, T \rightarrow \infty} n_b \sigma_{\min}\{\tilde{\Phi}_2(\Theta)\}$ exist and continuous with respect to Θ , where $\sigma_{\min}(M)$ is the smallest singular value of a matrix M . In addition, assume $\sigma_{\min}\{\tilde{\Phi}_1(\Theta^*)\} > 0$ and $\sigma_2(\Theta^*) > 0$.